People's Democratic Republic of Algeria
Ministry of Higher Education and Scientific Research

University M'Hamed BOUGARA – Boumerdes

Institute of Electrical and Electronic Engineering

Department of Electronics

Final Year Project Report Presented in Partial Fulfilment of
the Requirements for the Degree of the

MASTER

In **Telecommunication**

Option: **Telecommunications**

Title:

Design and Analysis of a Dual-Band Monopole Antenna for RFID applications

Presented by:

- **LAMINI Ikram**

Supervisor:

Dr. K. DJAFRI

Registration Number: ...../2023

Acknowledgment

Whatever has been accomplished and whatever has been the produced is all thanks to ALLAH and his guidance and gracious blessings and for leading us through rough situations when it seemed impossible to get out of there, all along our lives.

I am delighted to express my greatest gratitude and appreciation to those whom I have received academic support and mental strength from. Ahead of them, my final year project's supervisor **Dr. K.DJAFRI** who followed this project from the very beginning till the very end. Her tremendous support ,enormous patience and guidance led us smoothly to the completion of the project.

Furthermore, I want to extent my thanks to the teachers and their valuable input and all the staff of the Institute of Electrical and Electronics Engineering (IEEE Ex: INELEC).

Not to forget my precious family members and loved ones who accompanied me throughout the whole five years journey and fed me with their unconditional love and help, and all of my friends for always being there for me.

Dedication

In the name of ALLAH, I genuinely would like to dedicate this thesis to my idols in life, my father Menouer and my mother Nassima whose unwavering support and encouragement have been the driving force behind my academic journey. Their love, sacrifice, and belief in my abilities have made me the person I am today. This thesis is a testament to their endless faith in me, and I am forever grateful for their presence in my life.

To my beloved sister Feriel who played a major role in uplifting my mood and the curing mental health and whom I always find by my side whatever, whenever, wherever and forever.

Also, all other family members, my brother Zakaria, my sisters Imene and Israa and a special shoutout to my uncles and their wives.

To my best friends B. Wissam, M. Dounia and S.Amira with whom I had great and unforgettable memories.

To my university friends B. Rania Yasmine and M. Nadjet whom I felt knowing for years.

We have had so much fun together.

Abstract

In this work, a comb-shaped monopole dual-band antenna for 2.4/5.8 GHz RFID application is presented and tested. The proposed antenna is composed of an F-shaped monopole and a three-element comb structure which occupies a compact size of 28 × 32.8 mm^2 including the ground plane. Intermediate structures, including Γ-shaped, F-shaped, and modified F-shaped monopole radiators , are extensively investigated. To reduce the size of the modified F-shaped structure and cover the 2.4/5.8 GHz RFID operation bands, a comb structure is loaded between the two horizontal arms of the F-shaped branch. By properly selecting the gap , length , width and the number of elements of this comb, dual-band operation and compact size can be achieved. The proposed antenna is prototyped and tested experimentally by measuring its input reflection coefficient. The experimental results shows that the proposed comb-shaped dual-band antenna is having an impedance bandwidth ($S_{11} \leq -10$ dB) of 1200 MHz from 2 to 3.2 GHz and 450 MHz from 5.55 to 6 GHz, respectively. Moreover, the proposed dual-band structure is also having omnidirectional radiation patterns which makes it well suited to be used in the intended applications.

Table of contents

List of figures

List of tables

List of abbreviations

2D Two-Dimensional.

3D Three-Dimensional.

BW Bandwidth.

EF Electric Field.

FNBW First Null Beamwidth.

FR-4 Flame Resistant 4.

GPS Global Positioning System.

GSM Global System for Mobile communication.

HPBW Half Power Beamwidth.

IT Information Technology.

MICs Microwave Integrated Circuits.

MMICs Monolithic Microwave Integrated Circuits.

MSA Microstrip antenna.

PCB Printed Circuit Board.

RFID Radio Frequency Identification.

Rx Receiving antenna.

SMA SubMiniature Version A.

Tx Transmitting antenna.

VNA Vector Network Analyzer.

VSWR Voltage Standing Wave Ratio.

List of symbols

ϵ_r	relative permittivity.
h	substrate thickness.
λ_0	free space wavelength.
RL	Return loss.
Γ	Reflection coefficient.
S_{11}	scattering parameter (reflection coefficient).
Z_{in}	the input impedance of the antenna.
Z_0	the characteristic impedance of the transmission (feed) line.
f_H	low cutoff frequency.
f_L	high cutoff frequency.
D	directivity.
D_{max}	maximum directivity.
$U(\theta, \phi)$	radiation intensity.
U_0	average radiation intensity.
P_{in}	total input (accepted)power.
P_{rad}	radiated power.
G	gain.
e_{cd}	radiation efficiency.
Z_A	antenna's input impedance.
R_A	real part of antenna input impedance.
X_A	imaginary part.
R_r	active or radiation power in the far field.
R_L	losses from the material and the dielectric.
ϕ	the elevation angle.
θ	the azimuth angle.
dB	decibel scale.
dB_i	decibels relative to isotropic.
$\log_{10}$	decimal logarithm (logarithm base 10).

General introduction

Due to the need to ensure communication throughout the world in every second, communication equipment has evolved in recent years to become the most sensitive technologies [1], shaped in a certain way where each shape is dedicated to specific application. In a communication system, the antenna is the most important element because it serves as both sending and receiving ends. However, its critical importance is highlighted in wireless communications [1]. Although the transmitting and receiving modes are of reversed process, both antennas (Tx/Rx) nonetheless have the same characteristics, substance, and attributes.

Microstrip antennas (MSAs) are a type of antennas that play a significant role in various domains since they are low cost, small size, light weight and easy to install [2]. They are considered as low-profile antenna and highly required in aircraft's related applications as in radar altimeters which consist of arrays of MSAs. Their field of application extends to mobile communications such as *Global System for Mobile communication* (GSM), satellite communications such as *Global Positioning System* (GPS), *Radio Frequency Identification* (RFID), television, broadcast radio and the list goes on [3].

As said above, one of MSAs' applications is RFID, and within an RFID system, the antenna is an integral part of it. Throughout this project, a comb-shaped dual band monopole MSA for RFID application performing at the two microwave frequencies 2.4 GHz and 5.8 GHz, is proposed and analyzed. The process of reaching the final design goes through four different stages. The design evolution starts with analyzing a Γ-shaped structure, then a simple F design is derived and investigated . Then, a vertical strip is attached at the extremity of upper horizontal branch of the F-shaped antenna and hence develop the modified F patch antenna. This antenna operates in the intended 2.4/5.8GHz RFID operation bands. Finally, a comb-shaped structure is introduced to reduce the overall antenna dimensions.

The report is of three chapters which include the following:

In Chapter 1, some of the basic notions of antennas in general besides special features of microstrip antennas, their privileges and applications, and an overview about the RFID system are presented.

In Chapter 2, the design and analysis of modified F-shaped antenna operating at 2.39\5.92 GHz is investigated. This structure has evolved from Γ shape to modified F shape going through simple F one, and at each stage a parametric study is carried out to observe the effect of each geometrical parameter on the return loss. Current distribution and radiation pattern are also simulated and studied.

In Chapter 3, to reduce the modified F-shaped antenna dimensions and maintain the operating frequency bands, a comb-shaped antenna is introduced. The proposed design operates in two bands covering widely the 2.4\5.8 GHz RFID application with an overall size of 28×32.8 mm^2. The effect of the comb elements is investigated and profoundly analyzed by observing the return loss responses and the operating bands. Besides this, surface current distribution, maximum gain and radiation and total efficiencies are investigated. To validate the technical proposal, the antenna is fabricated and tested and good agreement between the simulated and the measured results is observed. Finally, the proposed antenna is compared with antennas, operating in the same bands, reported in recent literature.

A conclusion is presented at the end of the report.

CHAPTER 1: Generalities on Microstrip Antennas

1.1 Microstrip antennas: history and construction

Although antennas existed since the 19th century, the attention it had since then made its development quicker. In the 1950's, as the scientists were aiming to work in higher frequency ranges, the small sized antennas came into their minds hence the idea of microstrip antennas. However, the early 1970's was the period when they were given the chance to be on the spot [4].

So, the basic idea behind an MSA was to print a thin metallic conducting strip or a patch ($t \ll \lambda_0$[1]) on a surface of a dielectric substrate with a thickness h ($h \ll \lambda_0$, $usually\ 0.003\lambda_0 \leq h \leq 0.005\lambda_0$) and a ground plane on the other side of it [2] , and all this can be illustrated in Fig 1.1. Photolithographic or printed circuits techniques are applied to construct MSAs because their radiation beam is relatively wide on broadside to the plane of substrate [4].

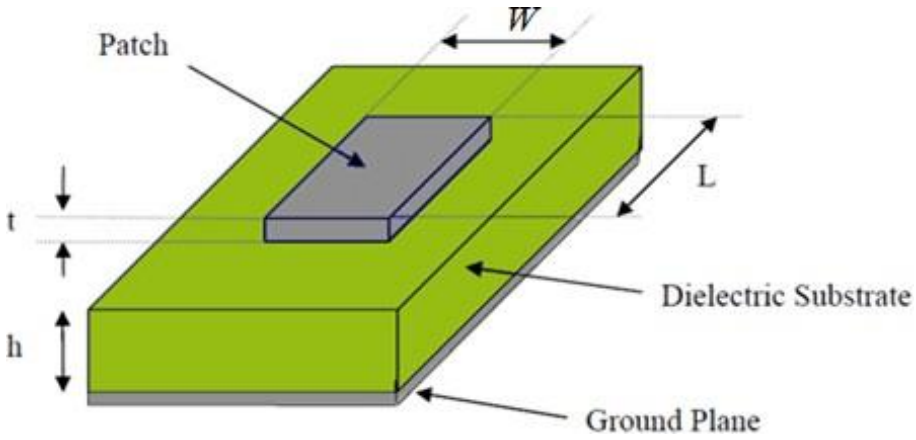

Fig 1.1. Basic structure of microstrip patch antenna [5].

The dielectric substrates used for the design of MSAs are various. However, the relative permittivity ϵ_r, is chosen from an interval of [2.2 to 12] [2]. It was found that the lower is ϵ_r, the higher is the thickness thus the better is the efficiency, the larger is the bandwidth and the bigger is the microstrip antenna and vice versa. So, for an antenna to perform well, ϵ_r must be the lowest within the interval.

1.2 Types of microstrip antennas

Microstrip patches can be of any continuous shape, but most used ones that are uniform like rectangular, square, circular, elliptical etc., because in one hand, they are easy to fabricate and in the other hand their analysis is simple. Fig 1.2 illustrates some of patch shapes.

[1] λ_0 : the free space wavelength.

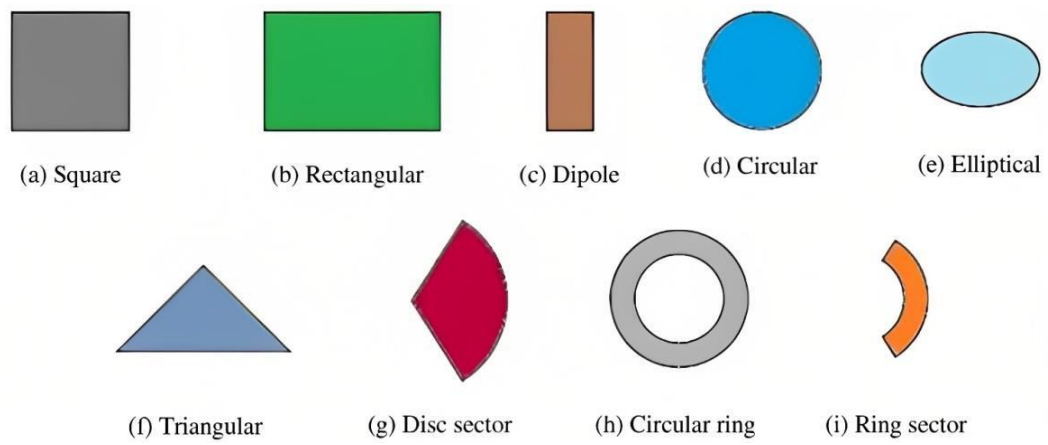

Fig 1.2. Common shapes of microstrip antennas [5].

1.3 Microstrip monopole antenna

In higher frequencies, Monopole antennas are a solution to the compromise between size, cost and simplicity. They are very required and an appropriate choice for dual-band or multi-band applications due to their simple structures, compact size, good impedance matching, ease of construction and omnidirectional radiation patterns [6].

1.4 Fundamental characteristics of microstrip antennas

In the upcoming sub-sections, basic properties of antennas in general are to be introduced.

1.4.1 Reflection coefficient and return loss

Return loss *RL* and reflection coefficient Γ are the most important parameters in any antenna, they indicate how well the antenna performs in the desired frequency. Γ is defined as the ratio of the reflected power from the antenna and the incident power from the source. Return loss corresponds to the scattering parameter S11 in dB, that is why its notation can be S11[dB] in the upcoming chapters.

RL is just Γ expressed in decibel as follows [7]:

$$RL = -20log_{10}|\Gamma| \tag{1.1}$$

Where Γ is the reflection coefficient and it is expressed in terms of input and characteristic impedances as [2]:

$$\Gamma = \frac{Z_{in}-Z_0}{Z_{in}+Z_0} \tag{1.2}$$

Where Z_{in} is the input impedance of the antenna.

And Z_0 is the characteristic impedance of the transmission (feed) line.

1.4.2 Voltage Standing Wave Ratio (VSWR)

VSWR is the acronym for voltage standing wave ratio. Its value indicates how much of impedance mismatch there is between the antenna's input and feed line. The lower the *VSWR*, the smaller the losses and the higher the power delivered to the antenna and vice versa. It is directly related to the reflection coefficient Γ. Its mathematical formula is given as [2, 7]:

$$VSWR = \frac{1+|\Gamma|}{1-|\Gamma|} \tag{1.3}$$

The practical value of VSWR must not exceed 1.3 and the ideal case is when $VSWR = 1$, no waves are reflected back to the source.

1.4.3 Frequency bandwidth (BW)

The bandwidth in general is the usable range of frequencies which includes the resonant or the operating frequency of the antenna (centralizes the band). The narrowness and the largeness of the *BW* depends on antenna's type and size.

In the case of microstrip antennas, the value *VSWR* identifies the *BW* which relies on the change in the impedance i.e., when the impedance mismatch occurs. It is usually determined from the graph of the return loss by the intersecting the -10 dB level or line with the S_{11} graph as illustrated in Fig 1.3 bellow.

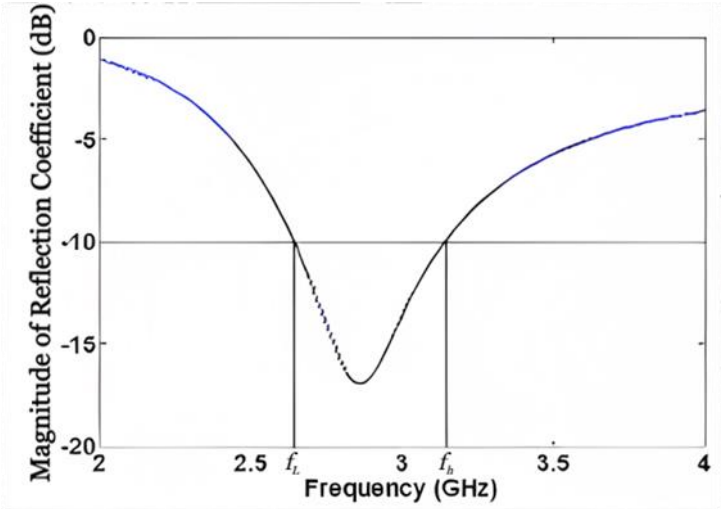

Fig 1.3. Bandwidth from -10 dB crossing in the graph of return loss [8].

The expression used to calculate the bandwidth is:

$$BW = f_H - f_L \tag{1.4}$$

Where f_H is the high cut-off frequency and f_L is the low one.

1.4.4 Directivity

The ratio of the radiation intensity in a specified direction $U(\theta, \phi)$ to that of an isotropic antenna is assigned to the directivity of an antenna. The average radiation intensity U_0 is given by dividing the antenna's radiated power P_{rad} by 4π [2].

$$D(\theta, \phi) = \frac{U(\theta,\phi)}{U_0} = \frac{4\pi\, U(\theta,\phi)}{P_{rad}} \tag{1.5}$$

If the direction is not indicated, the maximum radiation direction is considered which implies the maximum directivity and equation (1.5) becomes [2]:

$$D_{max} = \frac{4\pi\, U_{max}}{P_{rad}} \tag{1.6}$$

1.4.5 Gain

The gain is a parameter that is unique for each type of antenna. It is defined as the ratio of the radiation intensity in a certain direction to that resulted from an isotropic antenna radiation of the input power[2]. Transforming this into equation would give [2]:

$$G = 4\pi \frac{radiation\ intensity}{total\ input\ (accepted) power} = 4\pi \frac{U(\theta,\varphi)}{P_{in}} \tag{1.7}$$

When no direction is specified, the maximum radiation direction is taken.

The gain can be expressed in terms of directivity and radiation intensity. First, defining the radiation efficiency is just the radiated power divided by the input power [2].

$$\boldsymbol{e_{cd}} = \frac{P_{rad}}{P_{in}} \tag{1.8}$$

Hence:

$$G(\theta, \varphi) = \boldsymbol{e_{cd}} \left[4\pi \frac{U(\theta,\varphi)}{P_{in}}\right] = \boldsymbol{e_{cd}} D(\theta, \varphi) \tag{1.9}$$

1.4.6 Radiation pattern

It is known that the antenna starts radiating in its far field. when these radiations are plotted in space coordinates and converted into graphs, antenna's radiation pattern is resulted. It uses the normalized values of the field or power. Fig1.4 shows a set of space coordinates.

Two- and three-dimensional patterns (2D and 3D) are radiated power dispatched in space with respect to one's view along a path. 3D representation in practical circumstances is a combination of two 2D patterns.

[2] the radiation intensity of an isotropic antenna is just its total input power divided by 4π.

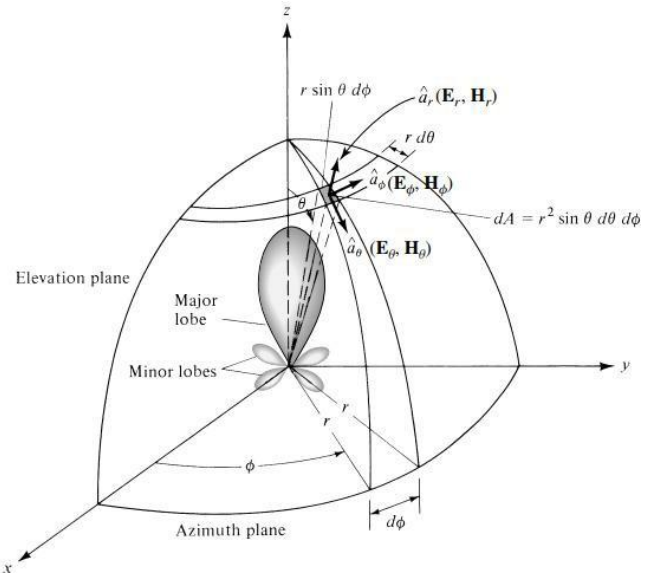

Fig 1.4. Suitable space coordinates for antenna analysis [2].

As previously stated, the pattern can either be a field or a power pattern in linear or decibel scales. In linear scale, field pattern is plotting the electric or magnetic fields' magnitudes as a function of angular space whereas power pattern is the plot of the square of either field's magnitudes versus the angular space. However, in the decibel scale, power pattern takes the values in dB.

1.4.7 Beamwidth

An antenna's radiation patterns consist of several lobes directed in certain direction. The lobe or the beam with the highest radiation level is called the main or major lobe, where a great amount of radiated power is located while others are called minor or secondary lobes, they are often undesirable. It is noted that lobes with an extreme opposite direction of the main lobe are referred to as back lobes. The direction of the main lobe determines the maximum directivity of the antenna [9].

The angular difference of two points in opposite sides of the main beam identifies the concept of the beamwidth. Half power beamwidth (HPBW) and first null beamwidth (FNBW) are the most useful beamwidth calculation [9]. These two interesting parameters are highly recommended in the study of antenna's characteristics for a wanted application.

This brief explanation can be seen in Fig 1.5

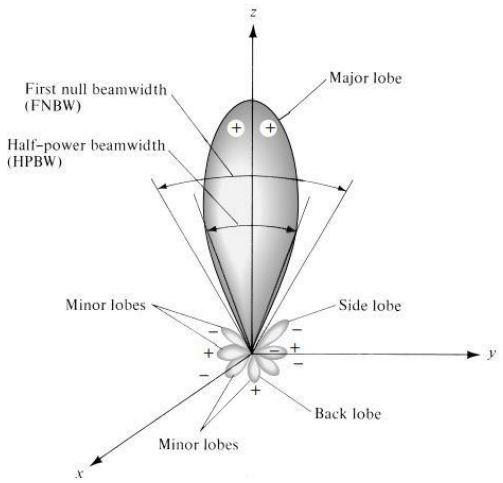

Fig 1.5. Antenna pattern's beamwidths and lobs [2].

1.4.8 Polarization

Polarization is defined by the radiated wave from the antenna. It is the variance of the direction and the magnitude electric field vector (EF) in time. Generally, the wave propagation direction is z- direction where the polarization is observed. There are mainly three classes of polarization: linear, circular, and elliptical [9].

a) Linear polarization

To say that an antenna is linearly polarized, the phase difference between the two components of the electric field vector (EF) must be zero (0) or multiple of π ($n\pi$) where $n = 1,2,3, \ldots$ hence, EF will either has only one component or two orthogonal components.

b) Circular polarization

If the EF vector movement is forming a circle, then the antenna has circular polarization. the two orthogonal components must have the same magnitude and the phase shift in this case must be either positive or negative multiples of $\frac{\pi}{2}$.

c) Elliptical polarization

When the antenna is neither linearly nor circularly polarized, it is said to be of an elliptical polarization. It can be noticed that the two previous types are special cases of elliptical polarization. The EF vector components can vary from one to two linear components. In case of two, they must be orthogonal and might be of same or different magnitudes. Same magnitude implies a phase shift different from multiples of $\frac{\pi}{2}$; so that

it would not be circular; and nonlinear polarization requires non-equal magnitude and imposes the phase shift other than multiples of π.

d) Co and cross polarization

Each antenna when radiating has co-polar and cross-polar components of its electric field. If the cross-polar coordinate is 20 dB less than the co-polar one, then it is of good polarization purity.

1.4.9 Input impedance

The input impedance as the name indicates is the impedance calculated at the entrance of an antenna. Its calculation requires a ratio of the voltage and the current of a pair of terminals or "the ratio of the appropriate components of the electric to magnetic fields at a point". The open circuit terminals' impedance is referred to as antenna's input impedance Z_A [2].

$$Z_A = R_A + jX_A \tag{1.10}$$

The real part of the input impedance R_A consists of the losses from the material and the dielectric referred to as R_L, and the active or radiation power in the far field R_r [2].

$$R_A = R_L + R_r \tag{1.11}$$

Whereas the imaginary part X_A is the radiation in the near zone.

The input impedance depends highly on the complexity of the feeding technique. The coaxial one is preferable because the proper location of the inner conductor results to the desired input impedance, and the cable is placed under the ground to minimize the coupling between the patch and the feedline [9].

1.5 Microstrip antennas advantages and disadvantages

Microstrip antennas are the best option in most of modern applications. However, this does not imply that they can only be beneficial without drawbacks. These two following sections will show some of their positive and negative aspects [2, 3].

1.5.1 Advantages

- ✓ Their construction is simple and of an affordable cost.
- ✓ Low profile antennas i.e., perform good regarding their small size.
- ✓ They are conformable with symmetrical or uniform (planar) surfaces and asymmetrical (non-planar) ones.
- ✓ Easy to access in case of problem, due to the photolithographic technique used when manufactured.

- ✓ MSAs are smoothly integrated into MICs and MMICs designs.
- ✓ They can perform in dual or triple frequency bands.

1.5.2 Disadvantages

- ✓ MSAs are poor in terms of efficiency due to material losses.
- ✓ They cannot support high power capacity.
- ✓ They lack polarization purity which implies high level of cross polarization.
- ✓ They have high quality factor Q (more than 100) and poor scan performance.
- ✓ They provide narrow frequency bandwidth (practically 1-5%) and small gain.

1.6 Feeding techniques

An antenna in general must be fed in order to start radiating, and the feeding techniques are various. When talking about the microstrip antennas, four major feeding processes are to be discussed. The patch can have a direct contact with the feed line in case of microstrip transmission line and coaxial feed, or an indirect one when dealing with electromagnetic and aperture coupling.

1.6.1 Microstrip transmission line

This kind of feeding, a conducting tiny strip is connecting the patch to its feed line and because this strip is printed on the same substrate as the patch, it gives it the planar configuration, so it is the advantage of this technique. However, its main drawback is the increase in the cross polar level and having undesirable radiation when the size of the patch and the feed are comparable and that mostly occurs in millimeter-wave range [3].

1.6.2 Coaxial feed

Coaxial or probe feeding process rooms over the conducting inner pin attached to the patch when the connector is soldered into the PCB. The ability to connect the feed line of this kind on any spot of the patch with just an impedance match makes it even a better technique [3]. It also has disadvantages like making the structure asymmetrical and maybe nonplanar. Also, it is difficult to design when the substrate's thickness is high ($h>0.02\lambda_0$) [2, 3].

1.6.3 Electromagnetic coupling

Also known as proximity coupling. It is placed in between the patch and the ground and separated by two dielectric media. Its privileges are the large bandwidth due to the increase in the substrate 's thickness, the elimination of unwanted radiation and the optimization of individual performances of the patch and the feed line since each of them

is connected to one dielectric medium. The problem that can be encountered in this type of feeding is the necessity of the exact alignment of the two dielectric material layers [3].

1.6.4 Aperture coupling

The concept of aperture coupling feeding way is as the name states it. Small aperture or a slot cut in ground side will excite the field from the microstrip line feed to be coupled to the radiating element. It is highlighted that the size and shape of the aperture will affect its performance. The centralized position of the aperture creates a sort of symmetry which leads to the reduction of cross-polarization [3]. The different discussed MSA feeding configurations are presented in Fig 1.6.

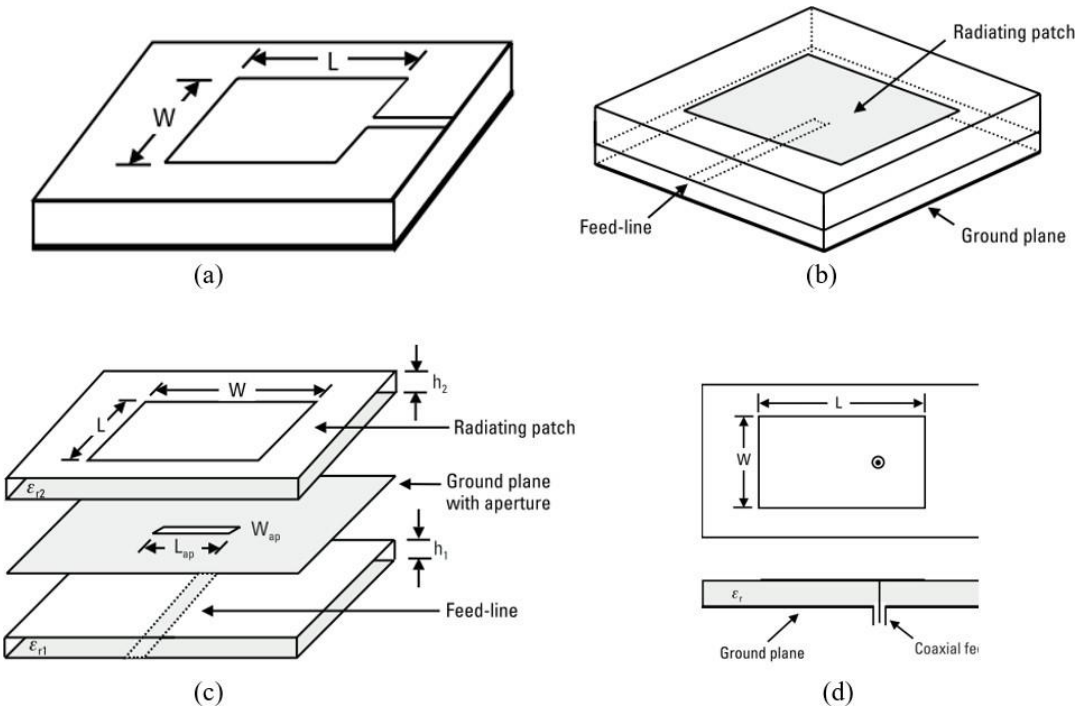

Fig 1.6. Rectangular microstrip patch fed by (a) microstrip line (b) electromagnetic coupling (c) aperture coupling and (d) coaxial/ probe feed [3].

1.7 Methods of analysis

Since the patch configuration are not unique and, in some cases, not familiar (non-uniform), the methods used to study these types of antennas properties are various, and for simplification of the calculations, the patch is considered as a 2D planar component [3]. Three major approaches are frequently used when handling the MSAs, transmission line, cavity, and full wave models.

1.7.1 Transmission line model

It is considered the simplest model of the three but the least efficient one and the non-suitable for coupling feeds. Its mechanism states that the patch is considered a transmission line with radiations along the length only with no consideration of the orthogonal direction of the propagation, and it result from the fringing fields at the patch extremities [2, 3].

1.7.2 Cavity model

Cavity model is more accurate way and more complex compared to the previous one [2]. Here, the separation between the ground and the microstrip patch is considered as cavity with magnetic walls around the periphery and electric ones from top to down. Due to the thinness of the patch, the field is distributed uniformly along the height of the cavity. To reduce the radiation effects in this type of model, boundary conditions in terms of impedance at the walls of the cavity are set [3].

1.7.3 Full wave model

Full-wave models can handle single element, finite and infinite arrays, stacked elements, arbitrary shaped elements, coupling, and elements of any size or shape. They are the most complicated models, and it gives the least physical insight. Methods of Moment is a method within this model which is largely used and specially in coupling feeding technique [2].

1.8 Microstrip antennas applications

Since MSAs are being available for manufacture in the market and with a low cost, it became highly demanded and used in various fields. Some of its main applications are to be stated [3].

- GPS and satellite communications.
- Air and marital navigation.
- Blind landing systems.
- Radar and proximity fuses in missiles.
- Broadcast, Radio, and mobile communication.
- RFID application.

1.9 RFID technology

Simply stands for **R**adio **F**requency **Id**entification. As the name refers to; it uses frequencies or electromagnetic waves to identify a certain object which should have an RFID tag attached to it. It was first used in World War II to distinguish the enemy's aircrafts from their own. The whole RFID system consists of a tag, a reader (or interrogator), an antenna, a middleware and application.

The information and content in the tag are read by the antenna and it is converted to computer data by the reader throughout a radio frequency and all that happens when an induction is created between the RFID antenna and RFID tag. The data in the tag is accessed by the reader that transmits it to the middleware, and this will lead to the final stage of recognition or identification that is the data processing which is done at the RFID application system's level. The middleware is an integral part of RFID system specially on software side. Its importance is pointed out within a workplace where it serves as a link between RFID networks and IT systems [10].

RFID tags are of three natures: passive, semi passive and active. The difference between the three of them is that passive ones are not associated with batteries while the two others are, however, the semi active tag uses the battery only with RFID reader's presence. An RFID system is shown in Fig 1.7.

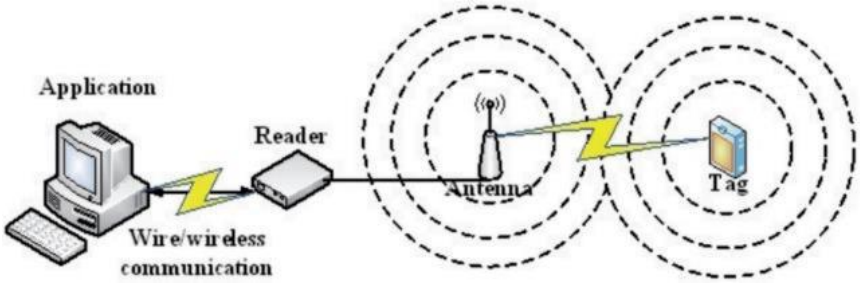

Fig 1.7. RFID system [10].

1.9.1 Advantages of RFID

The invention of such technology made great influence in the security sector. It is known to be the successor of the barcodes technology since it has some privileges over this latter, such as the contactless and the unnecessity of line of sight. RFID card is the most used model nowadays because it ensures added security and uniqueness of identification [10].

1.9.2 Uses of RFID

As referred to before, the fields of application of RFID systems are various. Some of them can be listed below [10, 11].

- ✓ Hospitals and health care: Inventory control, equipment tracking, out-of-bed detection and fall detection, personnel tracking, ensuring that patients receive the correct medications and medical devices, preventing the distribution of counterfeit drugs and medical devices, monitoring patients, and providing data for electronic medical records systems.
- ✓ Support of independent living of elderly and disabled persons.

- ✓ Environmental monitoring.
- ✓ Efficiency anti counterfeit.

1.9.3 RFID antenna

Amongst the different components of an RFID system, the antenna is the one of interest. This element can be designed to perform in low, high, ultra-high and microwave frequencies. Particular bandwidths and specific resonant frequencies are dedicated for RFID applications in each band. Tab 1.1 summarizes the different frequency ranges in each band.

Tab 1.1. Different frequency ranges for RFID application in different bands [12].

Band	Common Used Frequency	Type of Tag	Communication range		Allowed field strength transmission power
			Typical	Max.	
LF	125-134.2 KHz	Passive	20cm	100cm	72dB μA/m max.
HF	13.56 MHz	Passive and semi-passive	10cm	1.5m	60dB μA/m max.
UHF	433 MHz	Active	3m	10m	10–100 mW
	860 and 915 MHz	Active and passive	3m	15m	0.1–4 W
Microwave	2.4 and 5.8 GHz	Active and passive	3m	30m	0.5 – 4 W

1.10 Conclusion

In this first chapter, basic concepts about microstrip antennas and their privileges and drawbacks were given and an overview of an RFID system along with its fields of interest were presented the antenna design is discussed in the next chapter to achieve the dual band operation in the two microwave frequencies

CHAPTER 2: Modified F-Shaped Antenna

2.1 Introduction

The previous chapter introduced basic notions about antennas globally and microstrip ones precisely and a brief description of an RFID system thus the RFID antenna. In this chapter, a dual-band modified F-shaped patch antenna is designed and analyzed. The proposed structure is intended to work in two bands covering the 2.4\5.8 GHz RFID operating bands.

2.2 Γ-shaped microstrip antenna

In the process of reaching the final design and obtaining the aimed results, the design of the patch went through different stages. As a first stage, a Γ-shaped strip line is printed on FR-4 substrate with relative permittivity $\epsilon_r = 4.3$, a thickness $h = 1.6\ mm$ and a loss tangent of 0.025. The antenna is fed by transmission line, and it is connected to a 50 Ω SMA connector.

The proposed structure along with its different geometrical parameters is illustrated in Fig 2.1 and its dimensions are summarized in Tab 2.1.

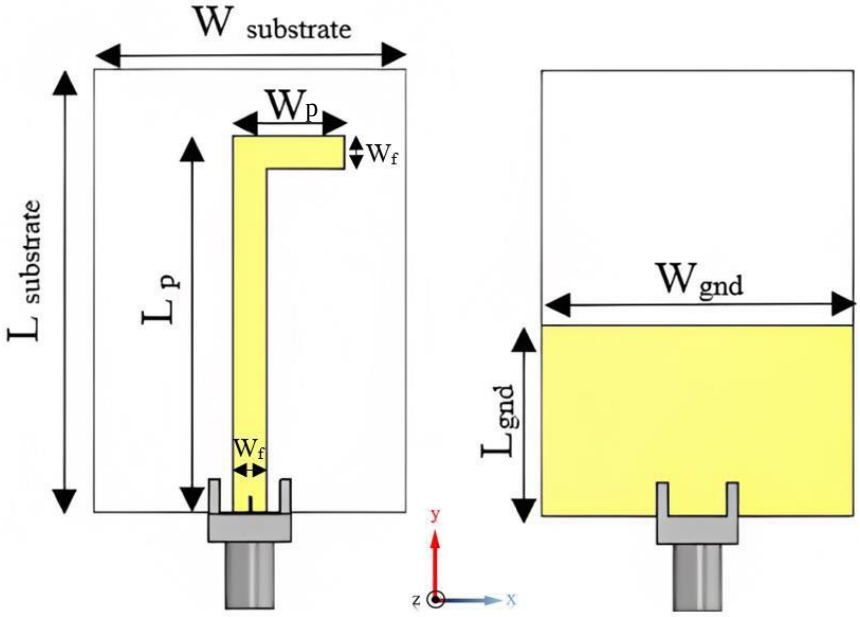

(a) (b)

Fig 2.1. Γ-shaped structure (a) top view (b) bottom view.

Tab 2.1. Γ-shaped antenna dimensions.

Parameter	$L_{substrate}$	L_{gnd}	L_p	$W_{substrate}$	W_{gnd}	W_f	W_p
Value (mm)	40	17	34	28	28	3	10

2.2.1 Simulated reflection coefficient

The simulated antenna reflection coefficient is presented in Fig 2.2. It can be noticed that this Γ- shaped design is a monoband antenna operating in the band (2.25 - 2.68 GHz) centered at 2.44 GHz with a return loss level of -23.26 dB.

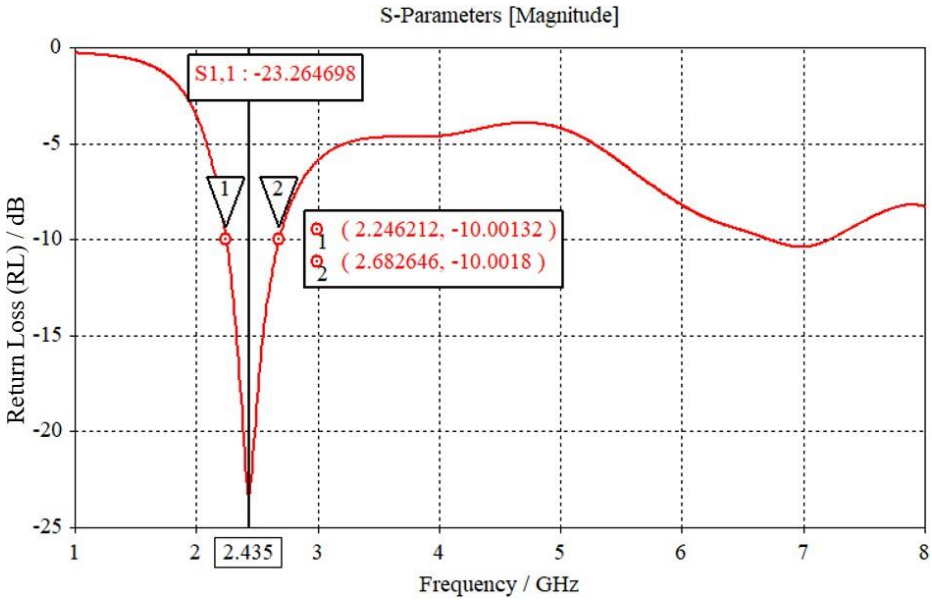

Fig 2.2. Simulated return loss of Γ structure.

2.3 Simple F-shaped patch antenna

To create the second band centered at 5.8 GHz, a rectangular strip of length L_2 and a width W_2 is attached to the Γ-shaped radiator. This modification, therefore, yields to the simple F structure presented in Fig 2.3.

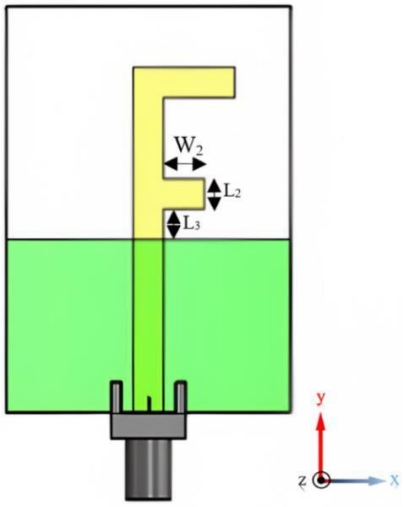

Fig 2.3. Simple F-shaped structure with L_2= L_3= 3 mm and W_2=4 mm.

2.3.1 Simulated return loss

Fig 2.4 shows the simulated return loss for this structure where it can be seen that the second band extending from 6.05 GHz to 7.23 GHz and resonating at 6.62 GHz with a return loss level of -22.43 dB. Regarding the first band, there is a small shift of resonant frequency from 2.44 GHz previously to 2.47 GHz for this structure and a small change in bandwidth to (2.28 – 2.73 GHz).

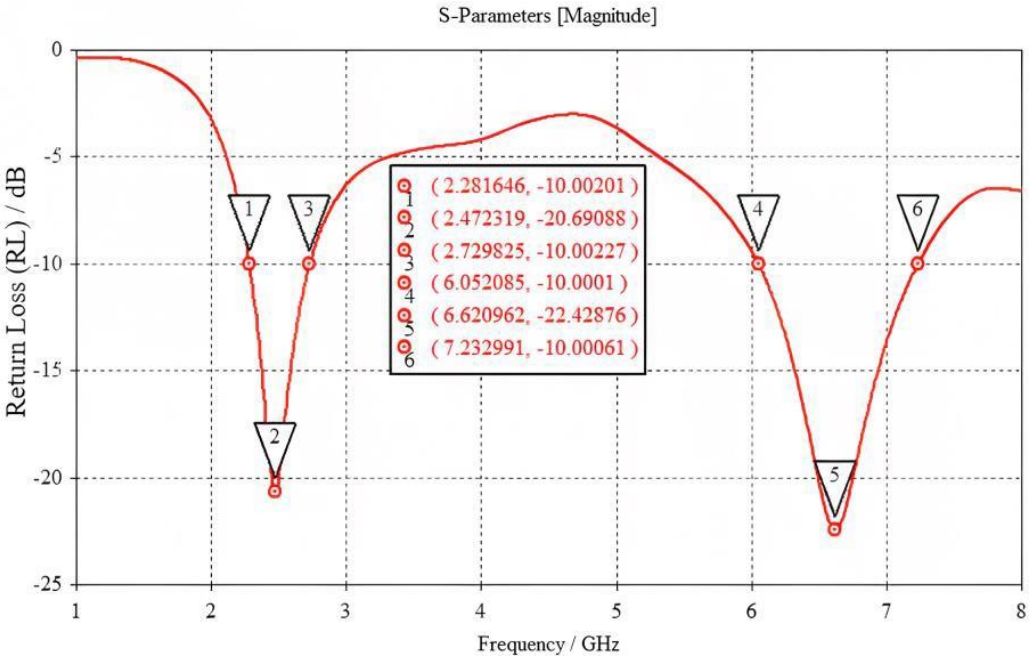

Fig 2.4. Simulated return loss for simple F-shaped antenna.

2.3.2 Parametric study

To see the effect of the added narrow strip on the reflection coefficient, a parametric study is done.

a) Effect of the width W_2

It can be deduced from Fig 2.5 that the width W_2 controls the second band and has no effect on the first band. It is noticed that the best matching and the closest frequency of the second resonance to 5.8 GHz are achieved when W_2= 4 mm.

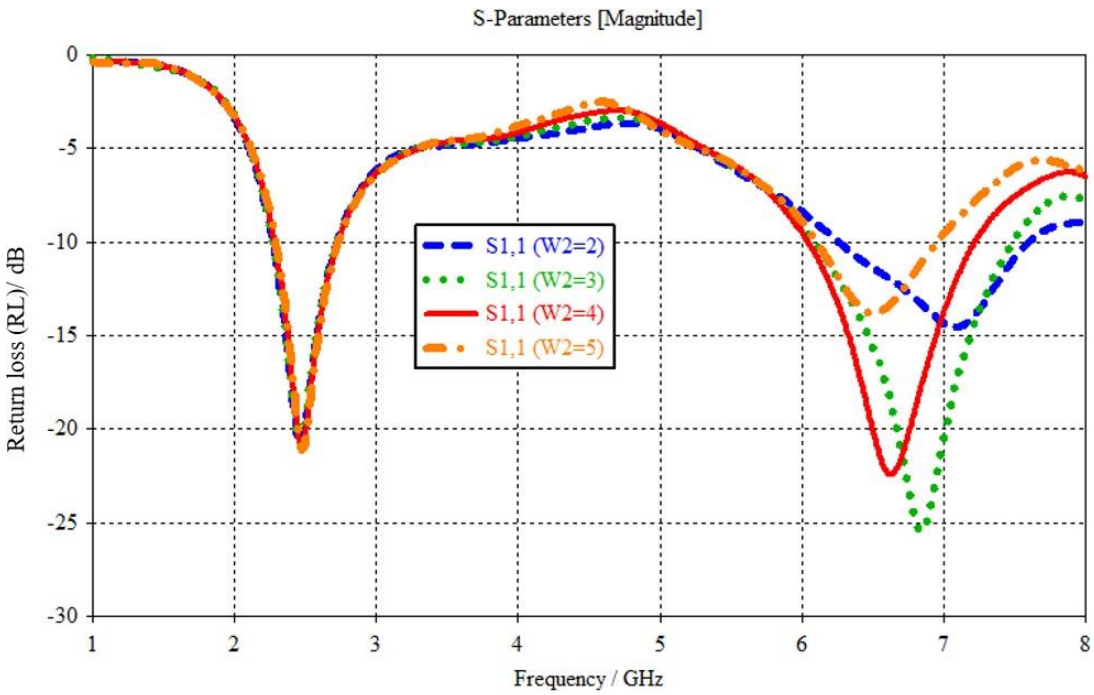

Fig 2.5. Simulated return loss results for different values of W_2.

2.4 Modified F-shaped structure

To centralize the resonant frequencies of the two bands to nearly 2.4 GHz and 5.8 GHz respectively, a vertical rectangular strip with width W_3 and length L_4 is added to the simple F-shaped antenna and the resulted structure is shown in Fig 2.6.

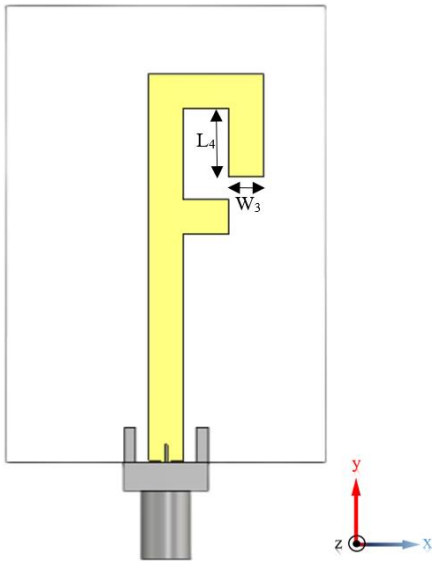

Fig 2.6. Modified F-shaped resonator with L_4= 6mm and W_3= 3mm.

2.4.1 Simulated return loss

The added strip in this structure has a remarkable impact on the second band as observed in Fig 2.7. The lower cutoff frequency of the second operating band is shifted down from 6.05 GHz to 5.15 GHz and the bandwidth is widened and extends to the end of the simulation range of frequencies, hence the operating frequency decreases from 6.62 GHz to 5.92 GHz. A shift of the first resonance from 2.47 GHz to 2.39 GHz is also noticed.

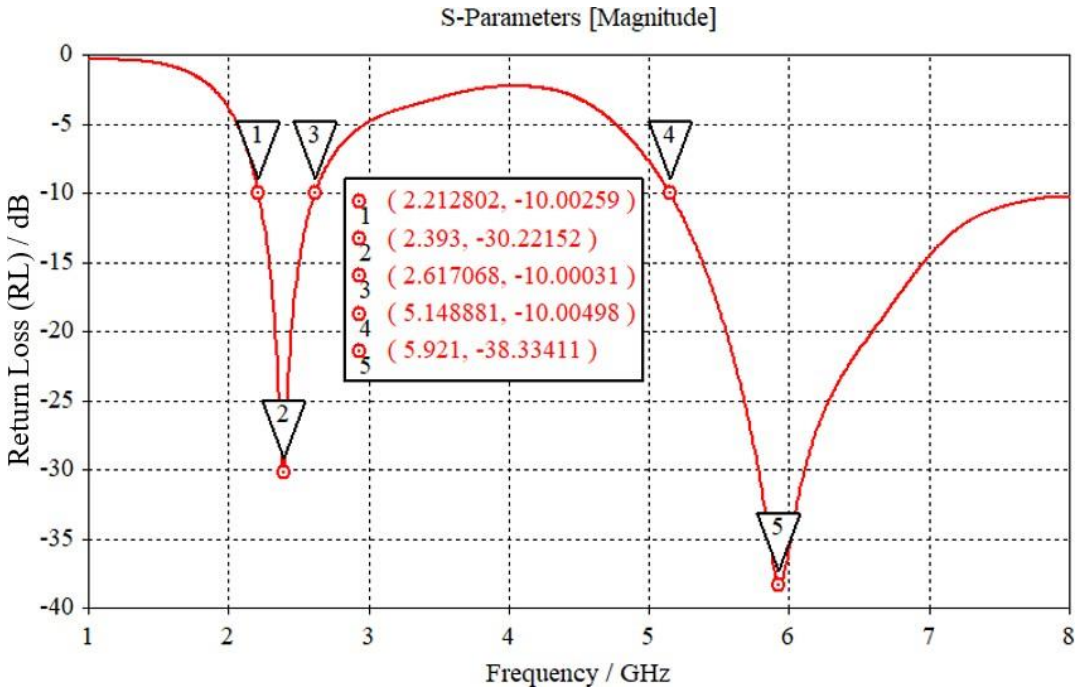

Fig 2.7. Simulated return loss of modified F-shaped structure.

2.4.2 Parametric study

A parametric study is performed to observe the effect of the vertical rectangular strip on the return loss.

a) Effect of the width W_3

The simulated return losses for different values of W_3 are depicted in Fig 2.8 and it is evident that it has an effect on both bands especially on the first one. By increasing W_3 from 1 to 4 mm, the first resonant frequency shifts from 2.56 GHz to 2.31 GHz. Good impedance matching with closest resonant frequencies to the intended RFID application in both bands, is achieved when W_3= 3 mm.

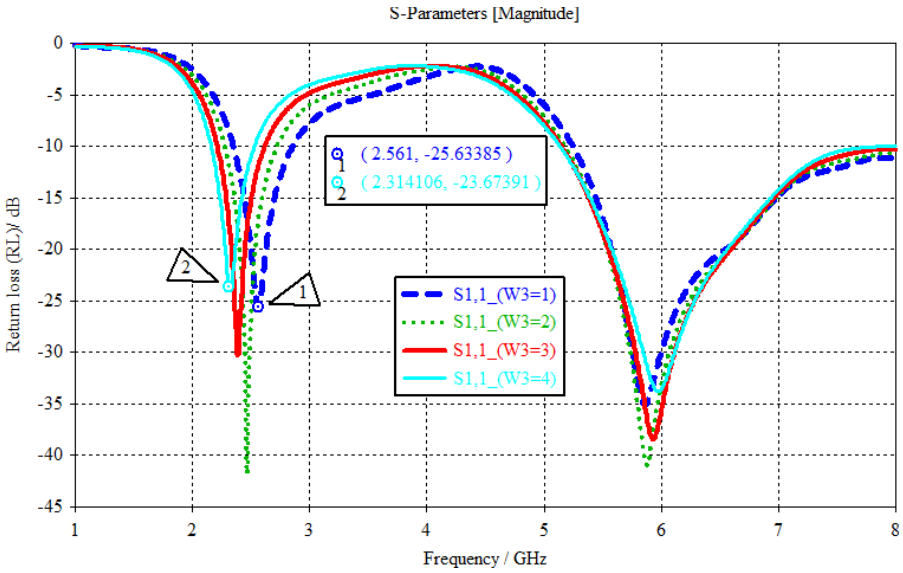

Fig 2.8. Simulated return losses for a set of W_3 values.

b) Effect of the vertical strip length L_4

Fig 2.9 displays the simulated return loss for different values of the vertical strip length L_4, and it has clearly a remarkable effect on the second band. Without ignoring the small impact on the first band, where increasing L_4 leads to the down shif of the frequencies. To have the best return loss level with the closest resonant frequency to 5.8 GHz, L_4= 6 mm is chosen.

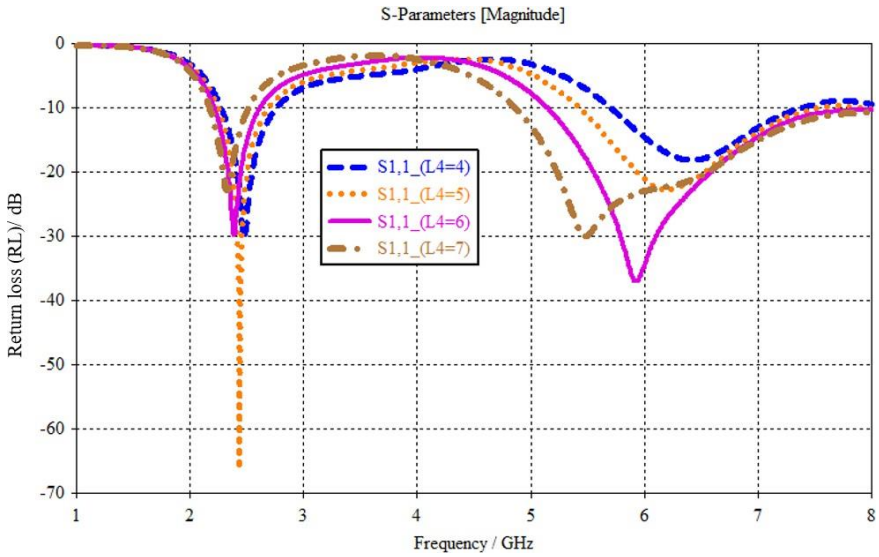

Fig 2.9. Simulated return losses for different values of L_4.

2.4.3 Current distribution

The concept of this dual band antenna is better understood by illustrating the surface current distributions at the desired resonant frequencies. Fig 2.10 and Fig 2.11 show the surface current distribution of the modified F-shaped antenna at 2.39 GHz and 5.92 GHz respectively. It is clearly observed that the current concentration is dense on the main strip and the vertical rectangular strip at 2.39 GHz whereas at 5.92 GHz, the current is dispatched all over the structure i.e., any change of any parameter would affect the second operating band.

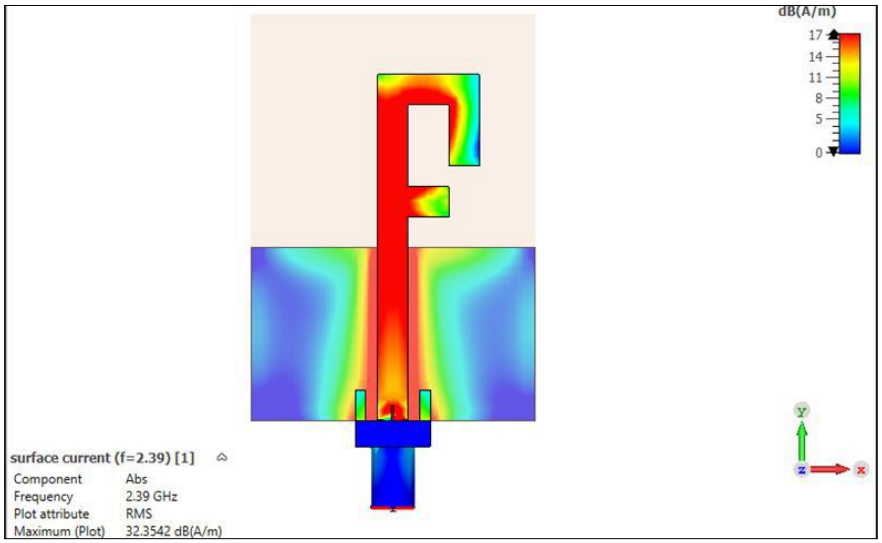

Fig 2.10. Simulated current distribution on the antenna at 2.39 GHz.

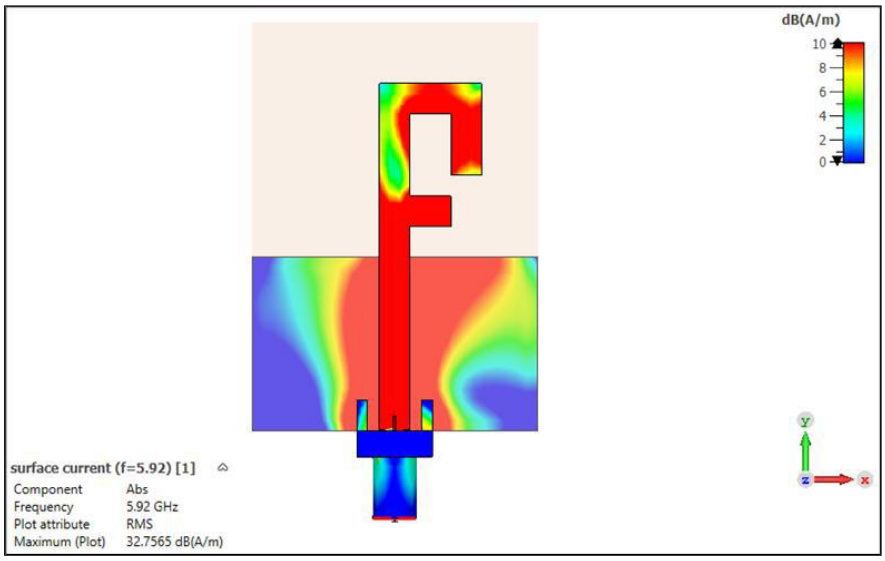

Fig 2.11. Simulated current distribution on the antenna at 5.92 GHz.

2.4.4 Maximum gain and efficiency

a) Maximum Gain

The maximum simulated gain sweep on the frequency range (1-8 GHz) is presented in Fig 2.12. It is seen that the maximum gain increases exclusively in the two operating bandwidths. The peak realized gain at the first resonance is 1.93 dB_i. Whereas at 5.92 GHz, the peak gain reaches 2.94 dB_i.

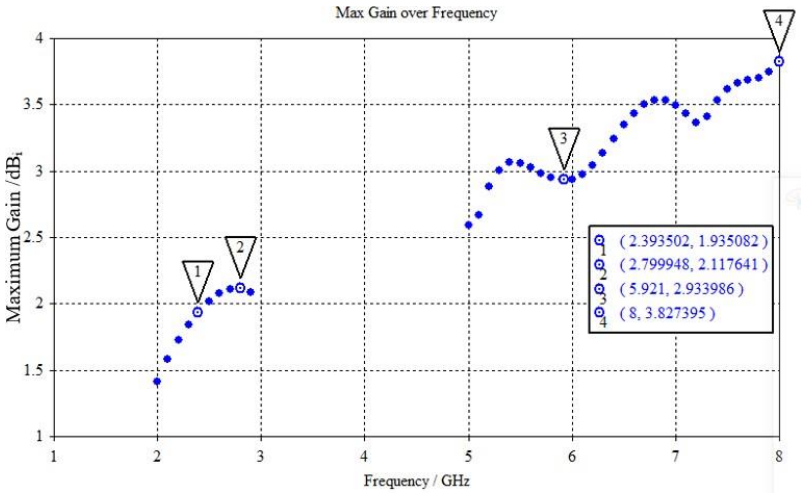

Fig 2.12. Antenna's peak gain versus frequency.

b) Efficiency

One of the important radiation characteristics is the efficiency and Fig 2.13 gives the variation of the radiation and total efficiencies in the two operating frequency bands . At the first operating frequency, about 90% radiation efficiency and 86.5% total efficiency are achieved. Similarly, at the second resonance, 79.6% radiation efficiency and 76.6% total efficiency are reached.

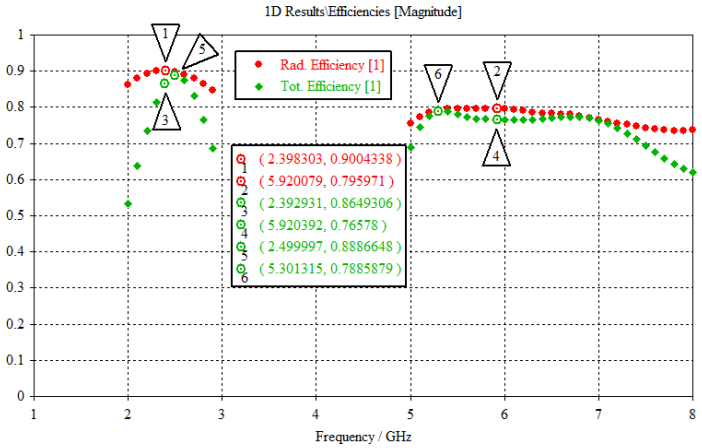

Fig 2.13. Simulated radiation and total efficiencies versus frequency.

2.4.5 Radiation pattern

The antenna is aligned along the Y-axis, what makes ϕ the polar angle while θ is the azimuth one. E-plane is obtained by fixing theta θ to $\frac{\pi}{2}$ that is the two-dimensional (x, y) plane, and H-plane is gotten by fixing ϕ to 0 i.e., the (x, z) plane. The E-plane and H-plane radiation patterns at 2.39 GHz and 5.92 GHz are illustrated in Fig 2.14 and Fig 2.15 respectively. According to simulations, in both operating frequencies, the resonator provides an omnidirectional pattern in the H-plane, however in the E-plane, the pattern has a figure eight.

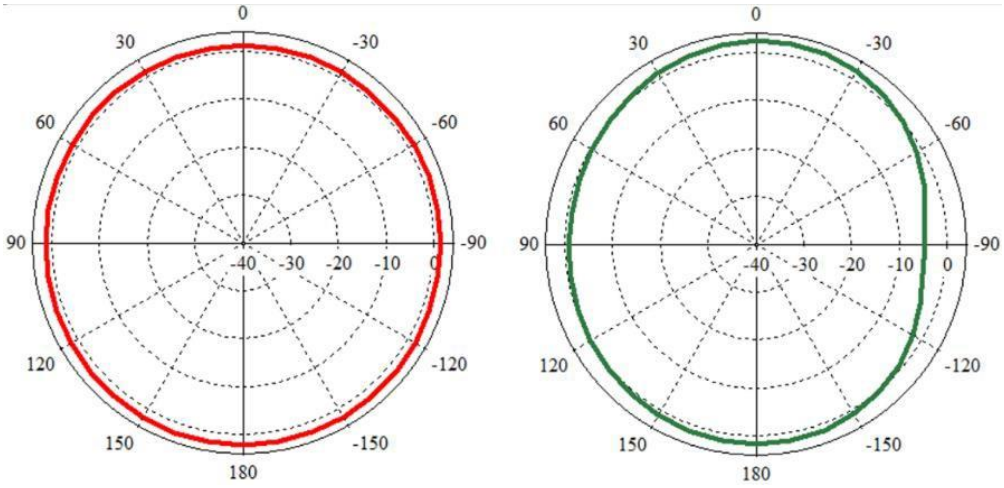

(a) (b)

Fig 2.14. The H-plane radiation pattern at (a) 2.39 GHz and (b) 5.92 GHz.

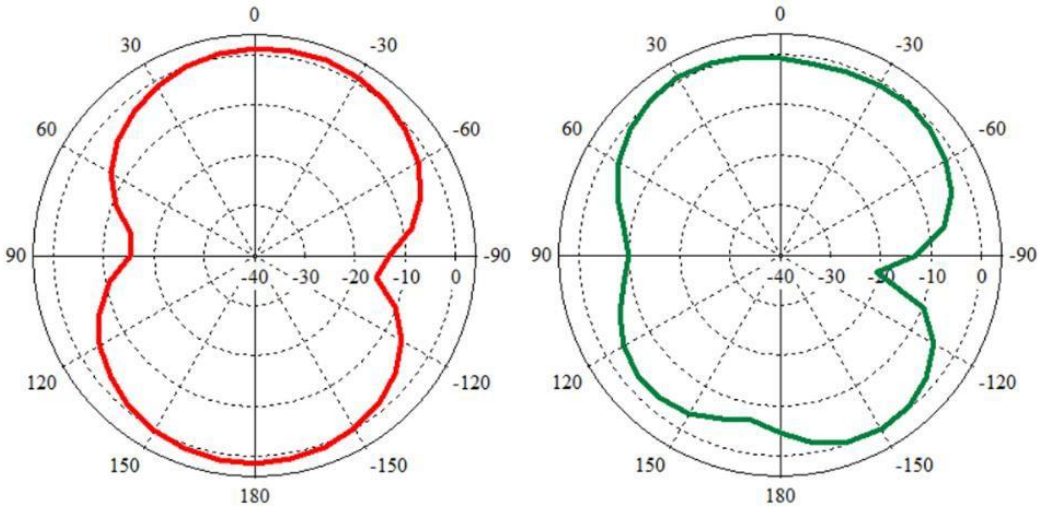

(a) (b)

Fig 2.15. The E-plane radiation pattern at (a) 2.39 GHz and (b) 5.92 GHz.

2.5 Comparison of the three structures

From the appearance perspective, the first patch shape was a Γ-shaped structure, then it became a simple F-shaped one and finally modified F-shaped patch and this design evolution is illustrated in Fig 2.16. The progress of reaching the corresponding microwave resonant frequencies for RFID application is seen through the frequency shifts of the bandwidths and the improvement in matching after adding the two arms to the first structure. This explanation is shown in Fig 2.17.

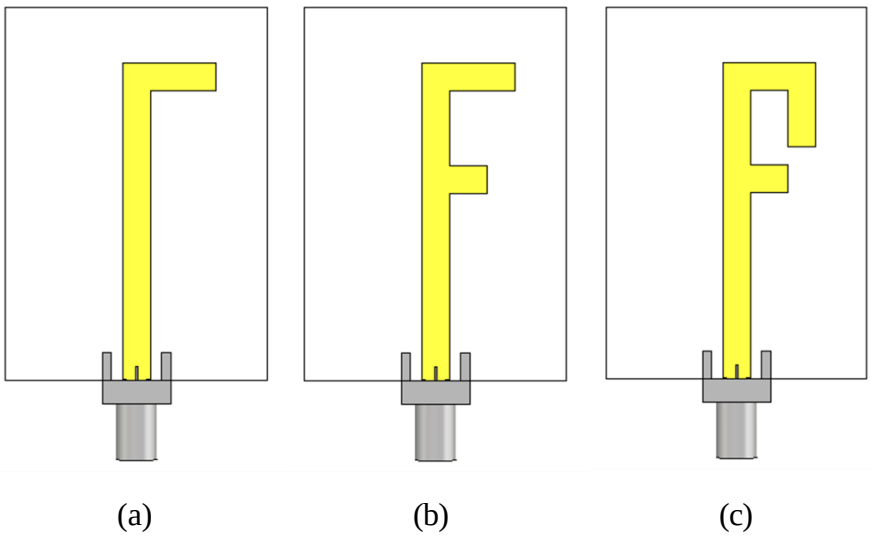

(a) (b) (c)

Fig 2.16. Patch shape evolution (a) Gamma (b) Simple F and (c) Modified F.

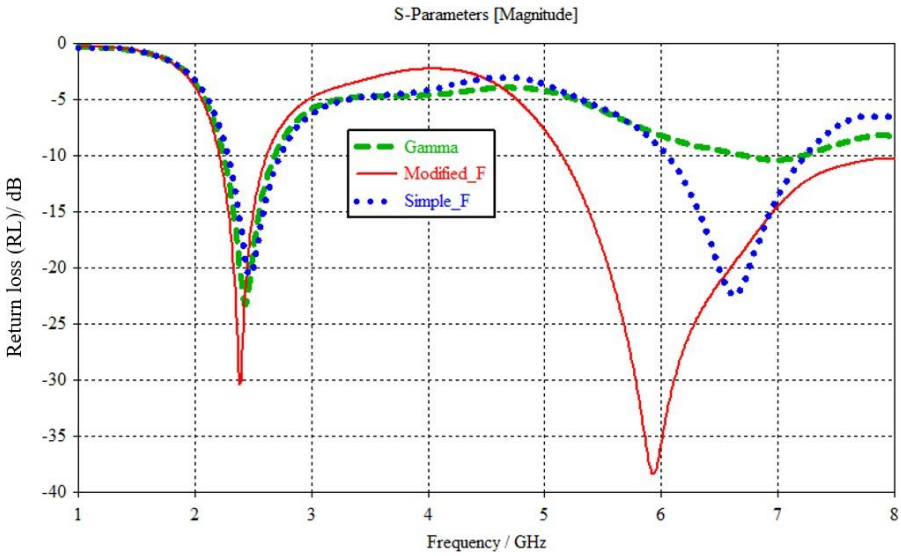

Fig 2.17. Simulated return losses for Γ- shaped, simple F-shaped and Modified F-shaped antenna.

2.6 Conclusion

Throughout this second chapter, an evolution of the antenna design from to one to finally modified F-shaped patch is presented. As a first stage, a Γ-shaped structure is introduced along with its corresponding return loss graph. A horizontal rectangular strip was added, and geometrical parameters values were assigned according to simulated return loss and parametric study to create a second band which led to the simple F structure. Another rectangular strip of a vertical alignment modified the previous structure and shifted down the resonant frequencies to the desired ones suitable for RFID application, and exclusively for this final structure, the current distribution, maximum gain, efficiencies and E and H planes were simulated and discussed. At the end of the chapter, a comparison among the three designs was made.

CHAPTER 3: Design and Analysis of a Comb-Shaped Monopole Antenna

3.1 Introduction

To reduce the size of the modified shape antenna, some modifications are made to the modified F- shaped antenna. The main modification is the introduction of a comb structure.

3.2 Comb-shaped antenna

In the process of reaching the final comb-shaped structure, the vertical rectangular strip presented in the modified F structure is eliminated and **n** horizontal rectangular strips with equal lengths $\mathbf{L_c}$ and widths $\mathbf{W_c}$ are attached. They are placed distant from each other as can be seen in Fig 3.1.

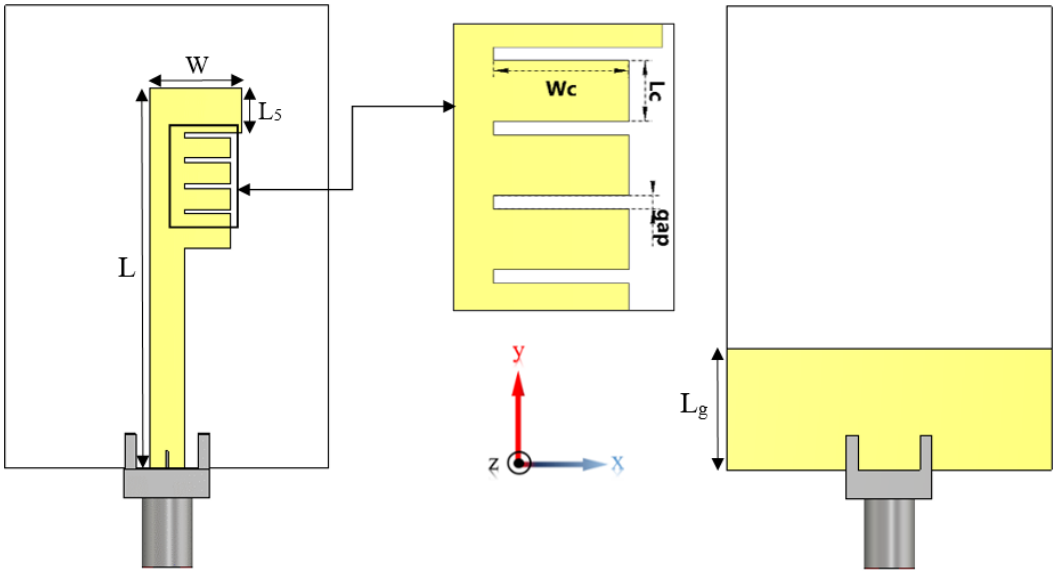

(a) (b)

Fig 3.1. Comb-shaped antenna structure (a) top view (b) back view.

Tab 3.1. Comb structure parameters' values.

Parameter	L	L_5	L_c	L_g	gap	W	W_c
Value (mm)	32.8	3.8	1.8	10.5	0.4	8	4

3.2.1 Simulated return loss

The simulated return loss for the comb-shaped antenna presented previously is presented in Fig 3.2. It is seen that the second band central frequency is exactly 5.8 GHz with a return loss level of -19.82 dB, this band extends nearly from 5.6 GHz to 6 GHz. Meanwhile, the first operating band (2.27 – 2.77 GHz) has 2.48 GHz as a resonant frequency with return loss level of -25.73 dB.

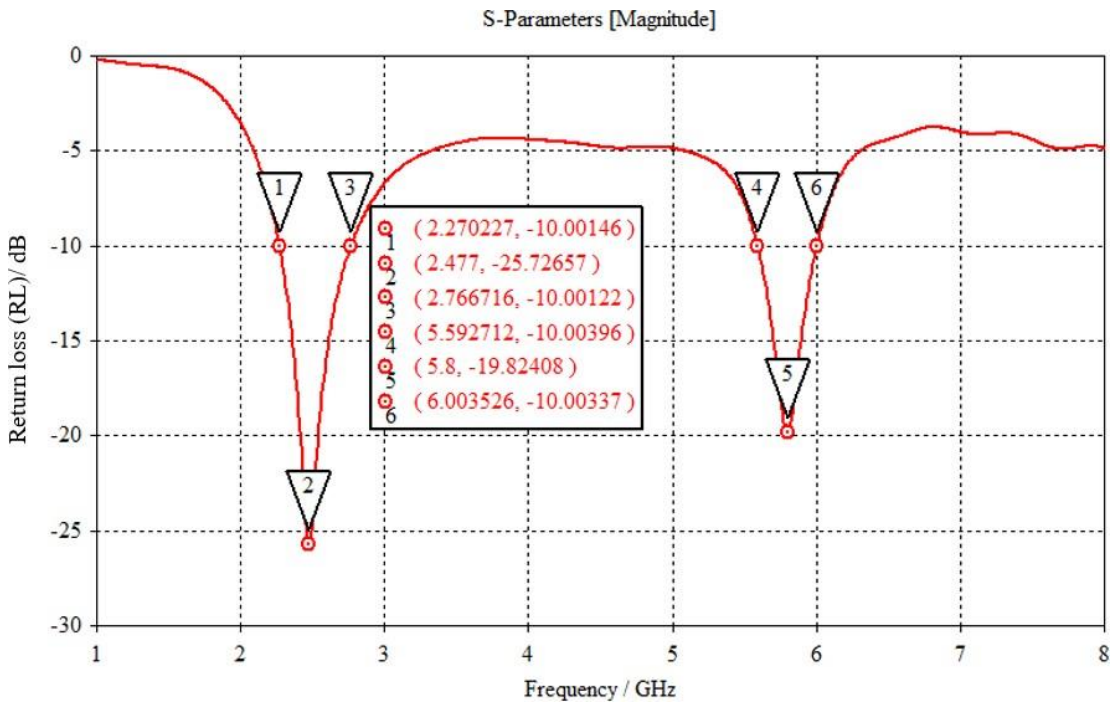

Fig 3.2. Simulated return loss of comb-shaped structure.

3.3 The effect of the comb structure on return loss

Since the vertical strip that modified the F structure was removed, extra strips must be added so that the frequency restabilizes to the RFID purpose one. To observe the effect of this comb structure

3.3.1 Effect of the spacing (gap) between the elements

Fixing the number of elements n = 5, width of one element Wc=4 mm and its length Lc = 0.9 mm, a parametric study of the gap is held. Fig 3.3 shows the different simulated return loss for each value of the gap. It is seen that it has a small effect regarding the second band and no effect of the first one, and the best result in terms of matching and closest resonant frequency to 5.8 GHz is obtained for gap = 0.4 mm.

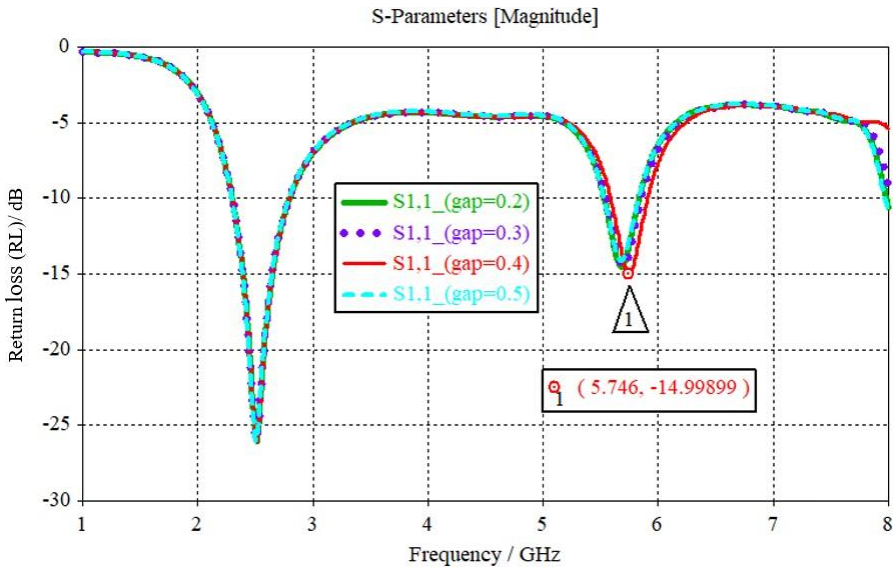

Fig 3.3. Simulated return losses for different values of the gap between elements.

3.3.2 Effect of the comb element length L_c

Previously, the values of the comb element's length L_c were assigned 0.9 mm and 0.3 mm respectively. Therefore, for the study of the effect of L_c, the comb element other parameters are kept constant (gap = 0.4 mm, n =3 and W_c=4 mm). In Fig 3.4, the simulated reflection coefficient for different values of L_c, from the set (1.6 – 1.9 mm) with a 0.1 mm step, is displayed. It can be seen from the results that the second operating band is slightly affected by the length L_c. Focusing on the graph of L_c = 1.8 mm, the second resonant frequency is perfectly matched to 5.8 GHz with a level of -19.82 dB.

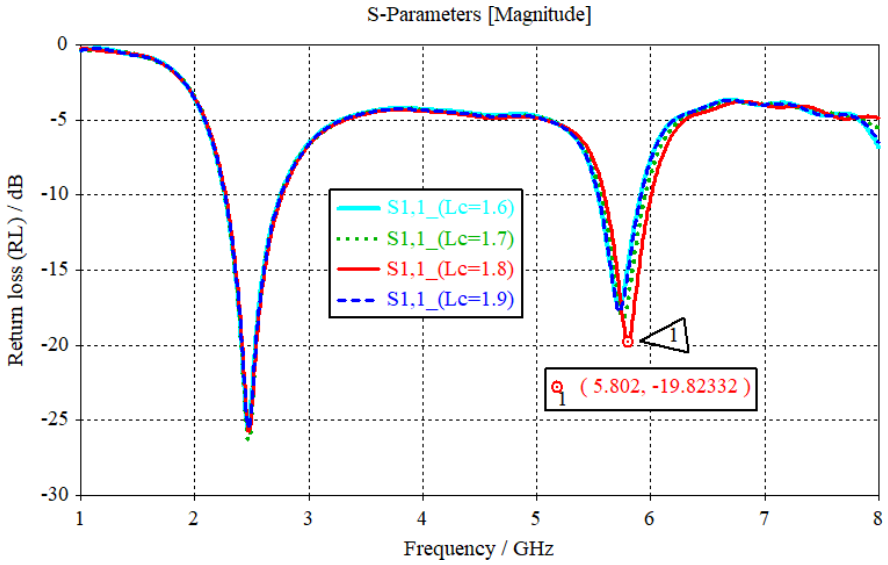

Fig 3.4. Simulated return losses for different values of the length L_c.

3.3.3 Effect of the comb element width W_c

In Fig 3.5, the different simulated return losses for different values of W_c from 2 to 5 mm are presented. Emphasizing on the graph of W_c = 4 mm, it shows a remarkable effect on the second band, and it is the most suitable value to cover the 5.8 GHz RFID operation.

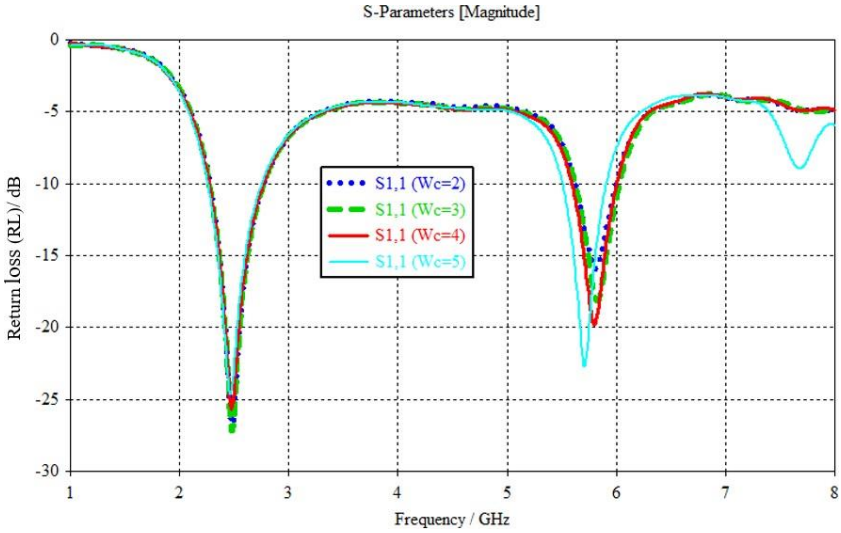

Fig 3.5. Simulated return losses for set of values of width W_c.

3.4 Effect of L_3 on the antenna return loss

In the design of modified F antenna, 3 mm was assigned to the separation of the patch from the ground L_3. Fig 3.6 shows the separation of the vertical strip from the ground for the comb structure. a set of values of L_3 are simulated and their corresponding return losses are illustrated in Fig 3.7. a length of 9.5 mm is adopted for the intended RFID requirements.

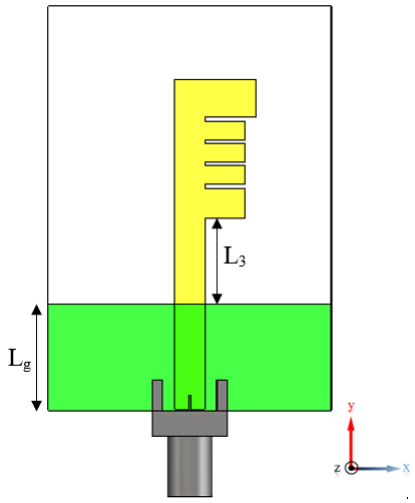

Fig 3.6. Comb structure with an illustration of the separation from the ground parameter.

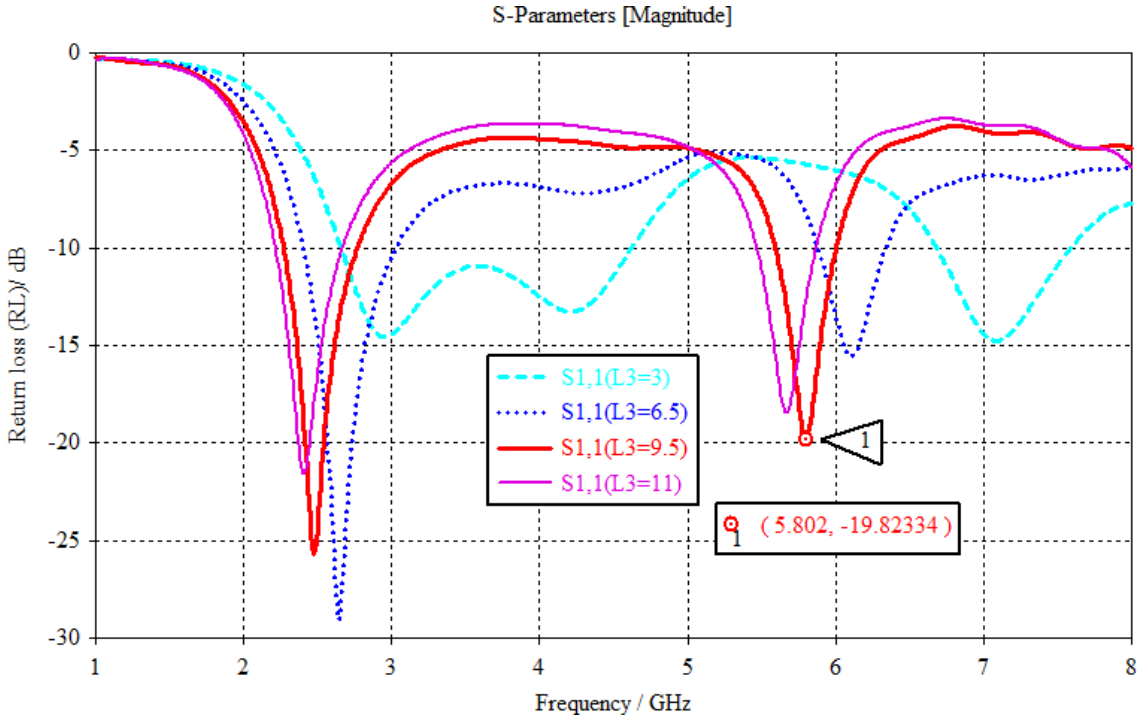

Fig 3.7. Simulated return loss graphs for different values of separation from the ground L_3.

3.5 Current distribution

The simulated surface current distribution of the proposed comb-shaped antenna at 2.48 GHz and 5.8 resonant frequencies are displayed in Fig 3.8 and Fig 3.9 respectively. At 2.48 GHz, the current is concentrated in the feedline and its density decreases as it reaches the edges. The comb elements have a small effect since the most of the current there tends towards zero. Whereas at 5.8 GHz, the current is gathered all over the patch including the comb structure, although it is less dense at the edges (the comb elements), any change at any spot will noticeably affect the second resonance. In the other hand, in the first resonant frequency, the current in the ground is dispatched symmetrically from the feedline and fades eventually when going towards the edges. Meanwhile at the second operating frequency, the current has higher intensities in comb patch structure and zeros at only the edges.

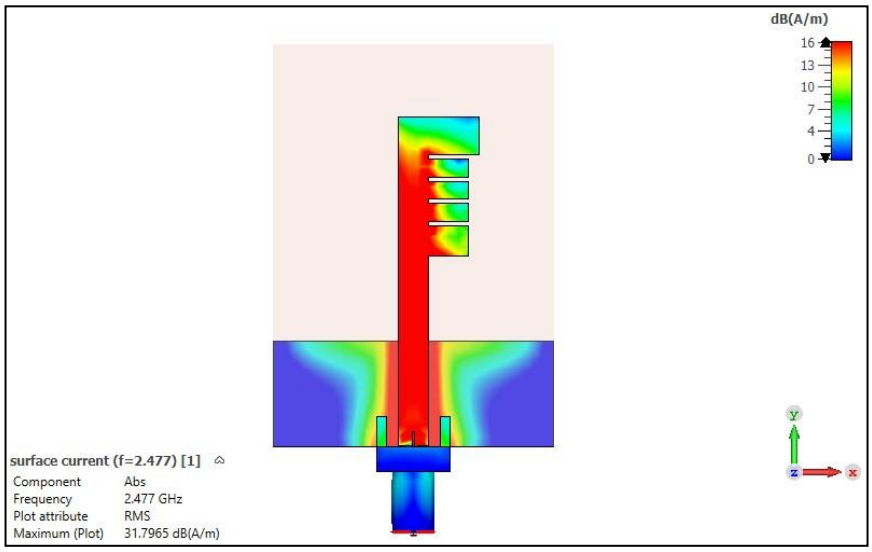

Fig 3.8. Simulated surface current on comb-shaped antenna at 2.48 GHz.

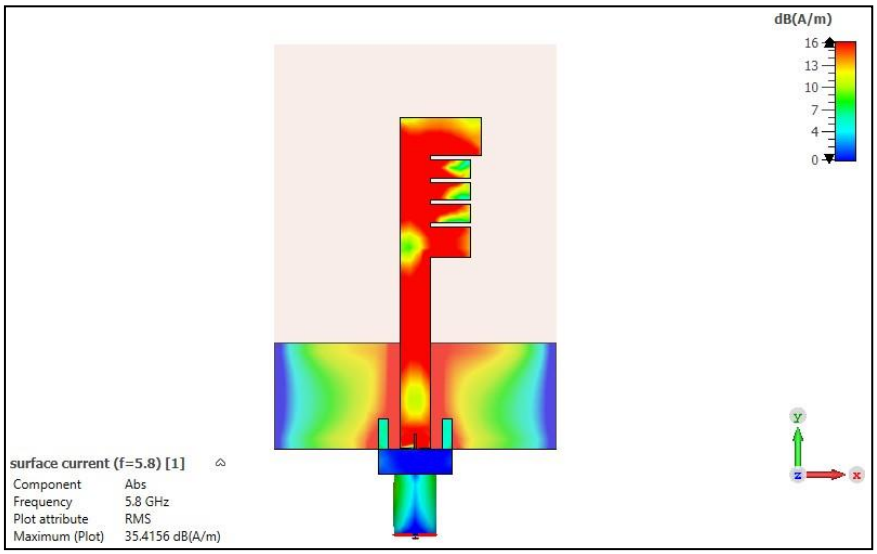

Fig 3.9. Simulated surface current on comb-shaped antenna at 5.8 GHz.

3.6 Maximum gain and efficiency

3.6.1 Maximum gain

The peak realized gain evaluated at the first and the second operating bands is in Fig 3.10. At the resonant frequencies 2.48 GHz and 5.8 GHz, the maximum gain reaches 1.85 dB_i and 3.09 dB_i respectively and it is noticed that it increases with the increase of the frequency from lower to higher cutoff frequencies.

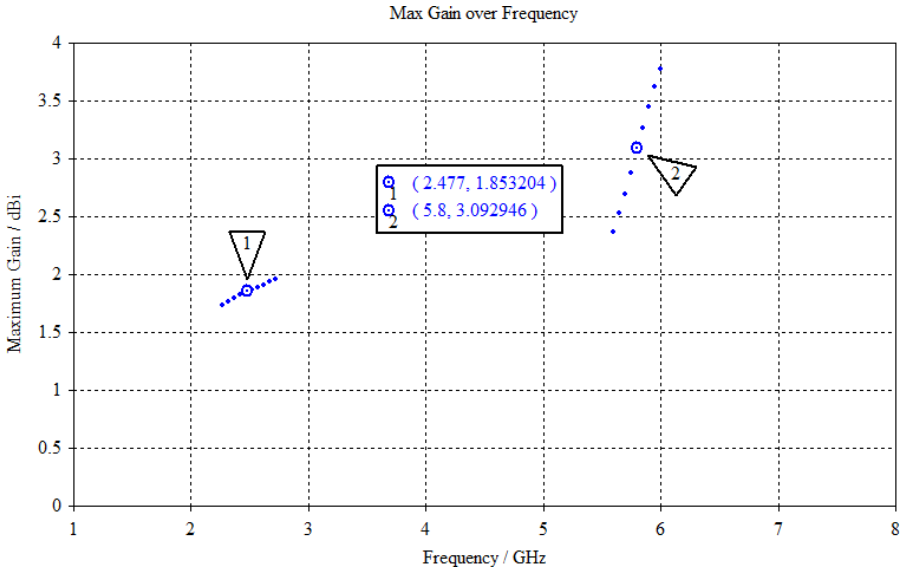

Fig 3.10. Antenna's peak gain versus frequency.

3.6.2 Efficiency

The radiation and total efficiencies are simulated, and their graphs are displayed in Fig 3.11. This figure indicates that the radiation efficiency reaches 92.3% at the first resonance and about 73.78% at the second. Meanwhile, a total efficiency percentage of 87.3%, 72.39% is recorded for 2.48 GHz and 5.8 GHz respectively.

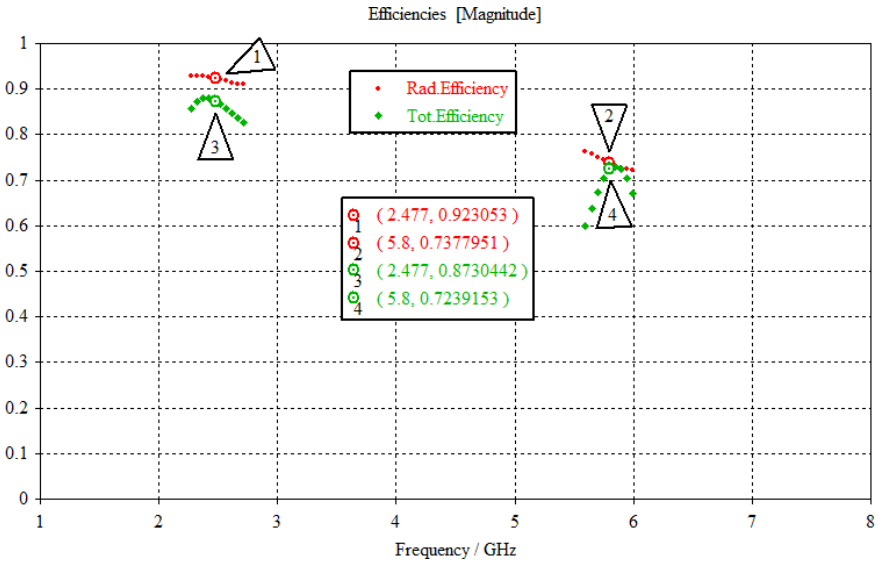

Fig 3.11. Simulated radiation and total efficiencies versus frequency.

3.7 Radiation pattern

Simulated radiation patterns in the E-and H-plane of the proposed antenna at frequencies 2.48 and 5.8 GHz are illustrated in Fig 3.12 and 3.13 respectively. The antenna radiates omnidirectionally

in both frequencies in the H-plane while in E-plane, an 8-shaped radiation pattern is provided at 2.48 GHz. and a radiation pattern which tends to be directional with side lobes where the first secondary lobe level is -2.2 dB at 5.8 GHz.

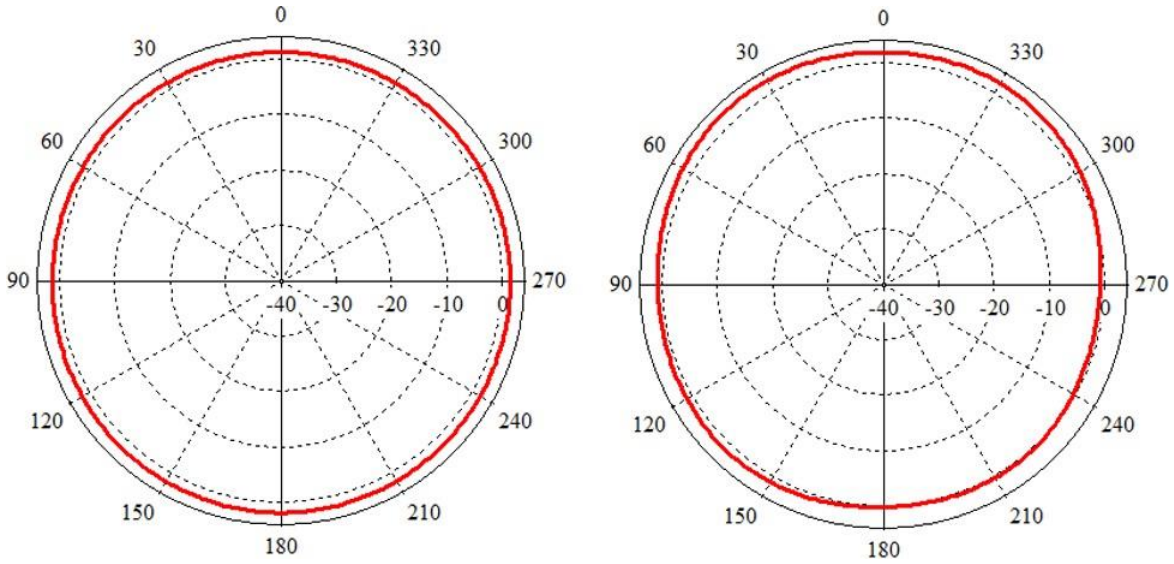

(a) (b)

Fig 3.12. The H-plane radiation pattern at (a) 2.48 GHz and (b) 5.8 GHz.

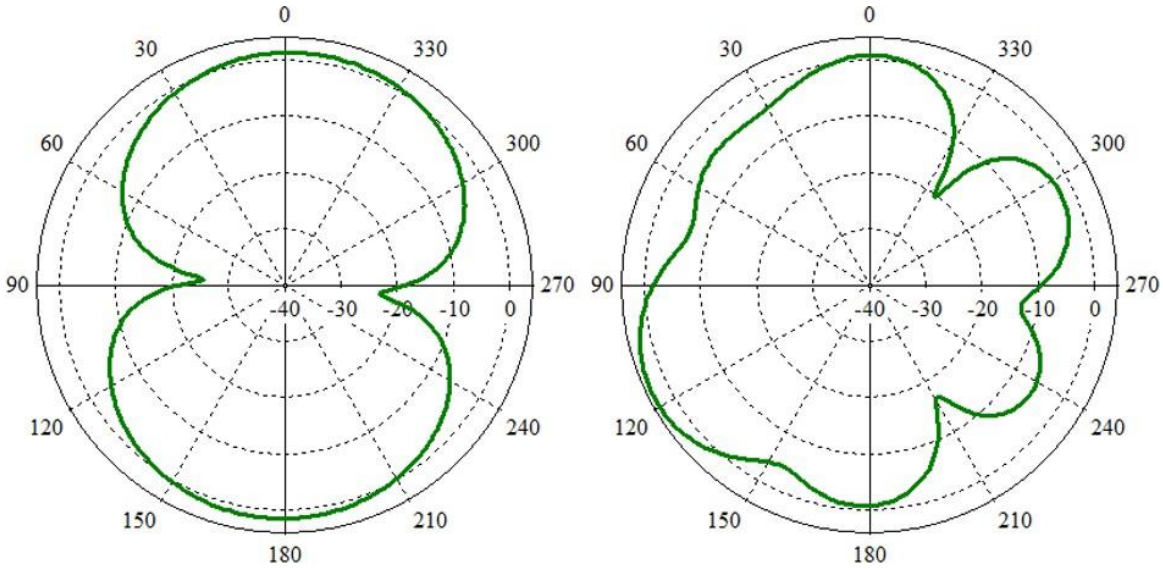

(a) (b)

Fig 3.13. The E-plane radiation pattern at (a) 2.48 GHz and (b) 5.8 GHz.

3.8 Comparison between the comb and antennas from recent literature

In Tab 3.2 a comparison is made between comb antenna and two reference antennas of recent literature regarding dual band monopole antennas working at microwave frequencies for RFID applications 2.4 GHz and 5.8 GHz. [13] is the first reference antenna (2020) and [14] is the second one (2019). Tab 3.2 shows that the proposed antenna have better results in terms compact size amongst the three. Also, it gives a larger bandwidth in the first band than the two others.

Tab 3.2. Comparison of the proposed comb antenna for RFID application with recent literature.

Antenna	Antenna size (L×W) (mm^2)	Operating Bands (GHz)	Bandwidth (MHz)	Resonant frequencies (GHz)	Footprint in terms of λ_0^2 (At the first resonance)
[13]	113 ×31	2.29 – 2.52 5.24 – 5.76	110 260	2.4 5.5	0.224
[14]	34 × 10	2.2 – 2.6 5.3 – 6.8	400 1500	2.6 5.8	0.027
Proposed comb	32.8 × 8	2 – 3.2 5.55 - 6	1200 450	2.5 5.76	0.019

3.9 Realization and testing of the comb-shaped antenna

The comb-shaped antenna was fabricated and tested by measuring the S_{11} parameter using the Vector Network Analyzer (VNA) scanning the range of frequencies from 100 kHz to 10 GHz. The photograph of the top and bottom views of the realized antenna is shown in Fig 3.14. Comparing the graphs of the measured and simulated reflection coefficient S_{11} in dB appearing in Fig 3.15, it is deduced that the results are in a good agreement especially in terms of the two resonant frequencies where measured values were recorded as 2.5 GHz and 5.76 GHz that are close to simulated values of 2.48 GHz and 5.8 GHz with an error percentage not exceeding 0.8 %. From the bandwidth perspective, the antenna practical performance gave a 1200 MHz bandwidth starting from 2 GHz, for the first band, and a 450 MHz bandwidth that extends from 5.5 GHz to 6 GHz, for the second band. The Two bandwidths cover the RFID microwave frequencies (2.4 GHz and 5.8 GHz). The difference between the measured and simulated results majorly depends on the manufacturing tolerances and precision, the non-exact value of the thickness and the dielectric

substrate relative permittivity, SMA connector, soldering effect and reflections from the surrounding objects.

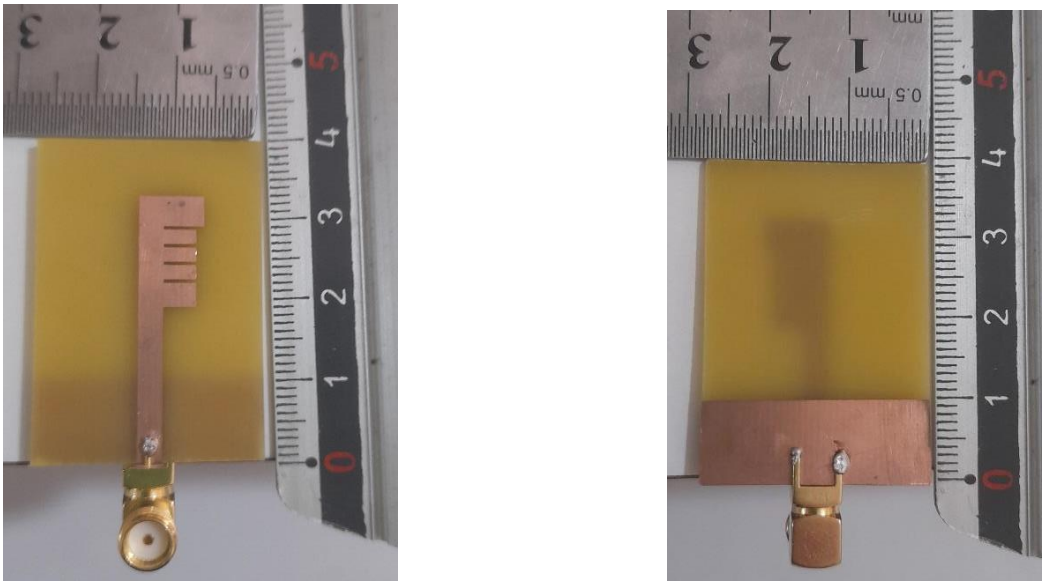

(a) (b)

Fig 3.14. Fabricated comb antenna (a) top view and (b) bottom view.

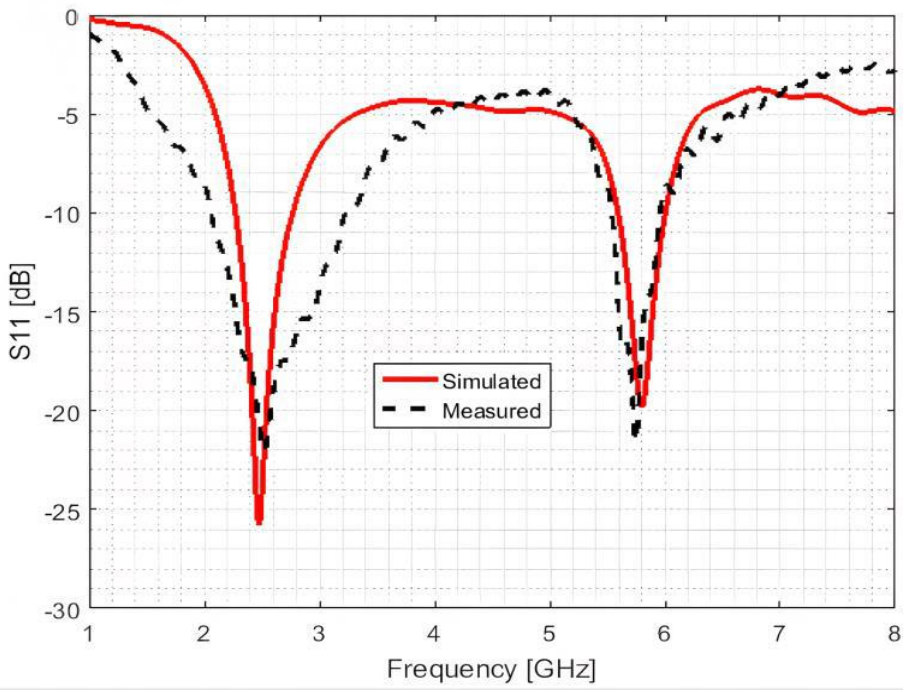

Fig 3.15. Simulated and measured S_{11} in dB versus frequency.

3.10 Conclusion

In this chapter a comb-shaped design is proposed to 2.4 and 5.8 GHz allocated to the RFID application. It was analyzed by studying each element's parameters and their effect on the S_{11} graph, to decide their final assigned value. The distribution of surface current on the patch and the ground were illustrated. Moreover, the maximum gain and efficiencies were plotted within the operating bands. Also, the antenna showed an omnidirectional radiation pattern in x-y plane and deformed 8-shaped directional pattern while radiating in y-z plane. Last but not least the proposed antenna was compared to two reference antennas in recent literature and at the end of the chapter, the antenna was realized and tested using VNA by plotting the magnitude of S_{11} in dB versus the frequency in GHz and the obtained measurements were satisfactory and good with simulations.

General conclusion

In this work, a compact comb-shaped microstrip monopole antenna is presented for 2.4/5.8 GHz RFID applications. The proposed geometry is printed on a low-cost FR-4 substrate having an overall dimension of $28 \times 32.8.mm^2$, which by attaching a three-element comb structure to an F-shaped monopole antenna, desired compact dimensions and dual frequency operation are achieved. The operating bands can be easily controlled by changing the dimension of the introduced comb .

To design the proposed comb-shaped antenna, three intermediate structures have been considered. The first design consists of an Γ-shaped monopole antenna. The simulated results have shown that the structure operate in a single frequency band extending from 2.25 to2.68 GHz centered at 2.47 GHz. To create another resonant frequency, a horizontal rectangular strip has been connected to the Γ-shaped structure to derive the F-shaped antenna. This resulted radiator operates in two bands extending from 2.28 to 2.47 GHz and 6.05 to 7.23 GHz. The first band covers the 2.4 GHz RFID operation band whereas the second band is not covering the 5.8 GHz RFID intended band. To cover this second band, a vertical strip has been connected to the upper extremity of the horizontal strip of the F-shaped design. The resulted structure is the modified F-shaped antenna which has shown dual-band operation covering perfectly the two intended bands with an overall size of $28 \times 34\ mm^2$.

To reduce the size of the modified F-shaped antenna without altering the operating frequency bands, a comb structure has been loaded between the horizontal arms of the F-shaped antenna. The obtained structure is a comb-shaped monopole radiator. This proposed structure has a compact size and work in two bands extending from 2 to 3.2 GHz and from 5.55 to 6 GHz covering widely the desired 2.4/5.8 GHz RFID operation bands. The simulated radiation pattern has shown that the proposed structure is having an omnidirectional pattern in both operating bands. To validate the proposed design, the comb-shaped antenna has been fabricated and its return loss has been measured and compared to the simulated results. Good agreement between the simulated and measured return losses is observed which make the proposed antenna is well suited to be used in the desired frequency bands.

References

[1] D. G. Fang, Antenna Theory and Microstrip Antennas, CRC Press, 2017.

[2] C. A. Balanis, Antenna Theory: Analysis and Design, Third ed., John Wiley & Sons, Inc., 2005.

[3] K. P. R. Girish Kumar, Broadband Microstrip Antennas, Artech House, INC, 2002.

[4] D. M. POZAR, "Microstrip antennas," *PROCEEDINGS OF THE IEEE*, vol. 80, no. 1, pp. 79-91, January 1992.

[5] S. Abdulkareem, "Design and Fabrication of Printed Fractal Slot Antennas for Dual-band Communication Applications," 2013. [Online]. Available: https://www.researchgate.net/figure/Figure-21-The-basis-structure-of-a-microstrip-patch-antenna-27_fig1_271530182. [Accessed 13 May 2023].

[6] J. Jung, W. Choi and a. J. Choi, "A Small Wideband Microstrip-fed Monopole Antenna," *IEEE MICROWAVE AND WIRELESS COMPONENTS LETTERS*, vol. 15, no. 10, pp. 703-705, October 2005.

[7] D. M. Pozar, Microwave Engineering, Fourth ed., John Wiley & Sons, Inc., 2012.

[8] [Online]. Available: https://www.quora.com/Why-s11-is-taken-below-10dB.

[9] P. A. AZRAR, "Antenna course notes," Institute of Electrical and Electronics Engineering IGEE (ex INELEC), University M'Hamed BOUGARA Boumerdes, Algeria, 2022.

[10] M. B. I. Reaz, Radio Frequency Identification from System to Applications, InTech, 2013.

[11] "https://www.fda.gov/," [Online]. Available: https://www.fda.gov/radiation-emitting-products/electromagnetic-compatibility-emc/radio-frequency-identification-rfid/. [Accessed 13 May 2023].

[12] "Categorizations of RFID tags by frequency and their allowed field strength," [Online]. Available: https://www.researchgate.net/publication/308167938_Use_of_Radio_Frequency_Identification_Systems_on_Animal_Monitoring#pf6. [Accessed 13 May 2023].

[13] A. R. Hassan, A. E.-A. Shady, S. Afaf and Z. Ahmed, "Dual-Band Printed Monopole Antenna Design," *ACES JOURNAL*, vol. 35, no. 10, pp. 1169-1175, October 2020.

[14] N. O. Parchin, H. J. Basherlou, R. A. A.-A. Noras and J. M., "Dual-Band Monopole Antenna for RFID Applications," *Future Internet*, vol. 11(2), no. 31, pp. 1-10, January 2019.